

# Impact of Size and Substitution Isomerism in Polycyclic Aromatic-Substituted Trialkoxysilanes on the Formation of Softenable Polysilsesquioxanes

Svenja Pohl, Markus Gallei, and Guido Kickelbick\*



Cite This: *Macromolecules* 2025, 58, 1298–1313



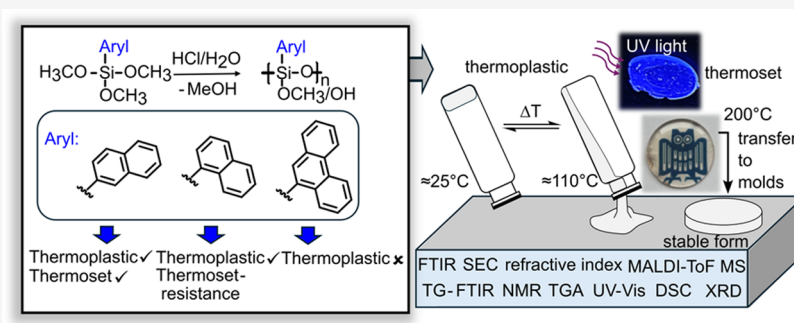
Read Online

ACCESS |

Metrics & More

Article Recommendations

Supporting Information



**ABSTRACT:** Polyphenylsilsesquioxanes are known to form glassy materials that can reversibly soften when heated above their glass transition temperature, with irreversible curing occurring upon a further temperature increase. In this study, the effects of the size and isomerism of polycyclic aromatic groups on the synthesis and structure of polysilsesquioxanes are investigated, with a focus on their thermoplastic and thermoset properties. Polysilsesquioxanes were synthesized by acid-catalyzed polycondensation using 1-naphthyl, 2-naphthyl, and 9-phenanthrenyltrimethoxysilanes. Characterization techniques, including spectroscopy, thermal analysis, mass determination, and powder X-ray diffraction, showed that steric hindrance by the aromatic groups significantly affects the degree of condensation, the formation of OH groups, and the nature of intra- or intermolecular condensation. Bulky phenanthrenyl groups hinder chain mobility and prevent detectable flow behavior, while 1- and 2-naphthyl groups enable the formation of thermoplastic materials with reversible softening. Notably, 2-naphthylsilsesquioxane undergoes irreversible curing at 200 °C, whereas 1-naphthylsilsesquioxane resists this transition. The incorporation of both polycyclic substituents not only preserves the characteristic thermoplastic behavior of melting gels but also introduces additional properties, such as fluorescence, a high thermal stability up to 460 °C and a high refractive index of 1.61, enhancing the potential of these materials for optical applications.

## INTRODUCTION

Polysilsesquioxanes ( $(\text{RSiO}_{1.5})_n$ ) exhibit an inorganic–organic hybrid composition consisting of an inorganic Si–O–Si backbone in which each Si atom is covalently bonded to three oxygen atoms and one organic substituent. This combination of functions imparts versatile properties to this class of compounds, including excellent heat stability, flame retardancy, resistance to environmental influences, ultralow dielectric constant, favorable mechanical properties, or biocompatibility.<sup>1–4</sup> Synthesis typically involves acid- or base-catalyzed hydrolysis and condensation reactions with organotrialkoxy- or organotrichlorosilanes.<sup>5</sup> The resulting structure varies depending on synthesis conditions such as temperature, monomer concentration, water content, pH value, and organic substituent nature, leading to ladder-like structures, open and closed cages, or random networks.<sup>6,7</sup>

A special material containing polyorganosilsesquioxanes was described from Masai et al. to provide an alternative to lead-

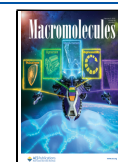
containing low-melting glasses.<sup>8</sup> The ability to exhibit a defined glass transition temperature ( $T_g$ ),<sup>9–11</sup> above which the polysilsesquioxane shows reflow behavior, i.e., it becomes flowable and moldable, has been used to produce transparent, hard, and glass-like thermoplastics. Although the materials did not show melting in the conventional sense and feature an amorphous structure, the term “melting gel” was established. Melting gels are produced from trialkoxysilanes or from a mixture of di- and trialkoxysilane, mostly with methyl and/or phenyl groups as organic substituents.<sup>12</sup> Most of them are hard and glass-like at room temperature and can be reversibly

**Received:** November 6, 2024

**Revised:** January 6, 2025

**Accepted:** January 20, 2025

**Published:** February 3, 2025



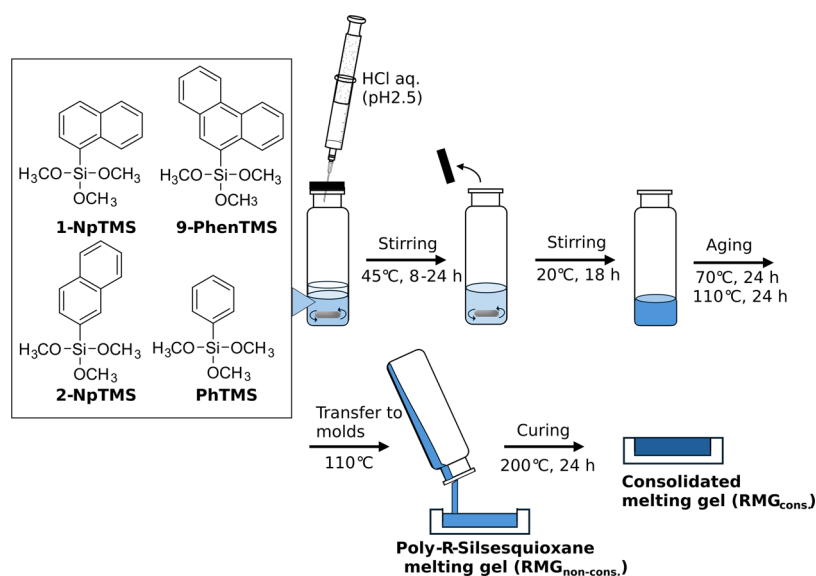


**Figure 1.** Scheme of the melting gel synthesis and structure of used trimethoxysilanes (TMS) with different aromatic substituents.

softened at around 110 °C. In this softened state, the material shows good processability similar to thermoplastics. At a consolidation temperature of  $\geq 130$  °C, melting gels cure irreversibly, and the resulting transparent, glassy material is neither softenable nor soluble. By varying the composition and type of monomers, the  $T_g$ , the viscosity, the consolidation temperature, and the refractive index can be adjusted.<sup>13–16</sup> These properties, as well as high thermal stability,<sup>17</sup> hydrophobic surface,<sup>18,19</sup> low gas permeability,<sup>20</sup> and transparency in a wide wavelength range,<sup>15,21</sup> make the materials interesting as hermetic barrier,<sup>20</sup> anticorrosive coatings,<sup>22</sup> for imprinted lithography,<sup>23</sup> in the field of water harvesting,<sup>24</sup> and for optoelectronic applications.<sup>25,26</sup>

When considering a softenable phenylsilsesquioxane as a model system for melting gels, the precursor gel is primarily composed of smaller oligomeric units, arranged in a random structure with partially ladder-like domains.<sup>27</sup> Stable OH and alkoxy groups (OR) interacting via H-bridges, as well as intra- and intermolecular  $\pi$ - $\pi$ -interactions of the phenyl groups, result in the extraordinary hardness, as well as the thermoplastic properties up to 110 °C. An increase in temperature results in condensation reactions of the interacting OH and OR groups and a reorientation of the structure to an increased number of ladder-like domains and a highly cross-linked material. Due to the high degree of cross-linking, no further softening of the material is possible.

Depending on the organic substituent, organotrialkoxysilanes show differences in their tendency to condense to softenable polysilsesquioxanes. *N*-alkyl chains as organic groups lead, according to the chain length, to highly cross-linked, insoluble solids, viscous oils, and even semicrystalline layered structures.<sup>28</sup> Only together with a comonomer like phenyl or methyltrialkoxysilane, *n*-alkyl substituents result in glass-like thermoplastics.<sup>20,29–31</sup> Recently, a poly(cyclohexyl)-silsesquioxane was described to form a stiff, transparent, softenable material.<sup>21</sup> In contrast to the conventional melting gels, it showed resistance to thermal curing, even after 6 h at 200 °C, which the authors attribute to the large steric hindrance of the cyclohexyl groups, preventing polycondensation between remaining Si–OH groups. A thermoset resistance of up to 300 °C was also observed by the incorporation of

benzyl groups in silsesquioxanes.<sup>10,32</sup> A further extension of the spacer between benzene and the siloxane backbone to the phenethyl group resulted in a viscous oil at room temperature.<sup>33</sup> The steric and electronic effects of the organic group seem to play an essential role in the formed structure and the softening and curing behavior of polysilsesquioxanes.

Since our group has previously shown that aromatic groups favor the formation of silanols<sup>34,35</sup> and that these seem to be a prerequisite for the formation of melting gels, we are interested in investigating the influence of the steric limits of aromatic substituents in polysilsesquioxanes and the formation of polymers with softening properties.

Aromatic compounds were mainly added to polysiloxanes in order to increase the refractive index for optoelectronic applications.<sup>26,36–38</sup> An influence of the type of the polycyclic group was also observed, both in the condensation tendency and in the fluorescence behavior.<sup>26</sup> The influence of polycyclic aromatic rings on the synthesis and structure of polysilsesquioxanes with no added comonomers has not yet been investigated in detail. We have recently shown that 1-naphthyltrimethoxysilane leads to softenable materials in a solvent-free, acid-catalyzed polycondensation reaction.<sup>27</sup> In the present study, we systematically investigated the influence of the isomerism and the size of the aromatic group on the hydrolysis and condensation behavior and consequently on the structure of the polysilsesquioxane as well as on resulting optical and thermal properties. Our aim is to extend the spectrum of melting gels by integrating further building blocks to add properties such as fluorescence or a high refractive index, which are associated with the incorporation of polycyclic aromatic compounds. Therefore, we condensed 1- and 2-naphthyltrimethoxysilane, as well as 9-phenanthryltrimethoxysilane via an acid-catalyzed polycondensation reaction analogous to a synthesis of a polyphenylsilsesquioxane melting gel (PhMG) described previously,<sup>27</sup> with the goal of forming aryl melting gels with polycyclic groups (Figure 1). The resulting structures were analyzed both after synthesis and after thermal treatment at 200 °C via nuclear magnetic resonance (NMR) spectroscopy, Fourier transform infrared (FTIR) spectroscopy, differential scanning calorimetry (DSC), thermogravimetric analysis (TGA), fluorescence spectroscopy, size

exclusion chromatography (SEC), matrix-assisted laser desorption/ionization time-of-flight mass spectrometry (MALDI-ToF MS), and powder X-ray diffraction (PXRD).

## EXPERIMENTAL SECTION

This section provides a description of the most important syntheses only; additional details on synthesis and characterization are available in the Supporting Information (SI).

**Melting Gel Synthesis.** The melting gels were prepared according to a modified previously described synthesis.<sup>27</sup>

**Naphthyl Melting Gel (NpMG).** 1-Naphthyltrimethoxysilane (2-naphthyltrimethoxysilane) (2 g, 8 mmol, 1 equiv) was stirred with aqueous HCl, pH 2.5 (0.217 mL, 1.5 equiv related to H<sub>2</sub>O) in a 20 mL sealed headspace vial at 45 °C for 8–24 h (600 rpm), until a homogenization of the two-phase mixture was visible. Afterward, the lid of the vessel was opened, and a significant increase in viscosity was observed over a stirring period of 18 h at room temperature. The byproducts, water and methanol, of the polycondensation reaction were subsequently removed by oven treatment at 70 and 110 °C for 24 h each, resulting in a transparent, glassy material at room temperature, which can be reversibly softened at 110 °C.

**9-Phenanthrenyl Melting Gel (9-PhenMG).** 9-Phenanthrenyltrimethoxysilane (0.3 g, 1 mmol, 1 equiv) was dissolved in acetone (2 mL) and stirred with aqueous HCl, pH 2.5 (0.168 mL, 3 equiv related to H<sub>2</sub>O) in a 20 mL sealed headspace vial at 45 °C for 24 h (600 rpm). Afterward, the lid of the vessel was opened, and the solvent was allowed to evaporate over a stirring period of 18 h at 45 °C. The byproducts, water and methanol, of the polycondensation reaction were subsequently removed from the gel by oven treatment at 70 and 110 °C for 24 h each, resulting in a yellowish, brittle solid.

**Melting Gel Consolidation.** For consolidation, the precursor gels were treated on Teflon plates at 200 °C for 24 h in a compartment dryer. The rigidity of the samples was tested at 200 °C by using a spatula. The material was cured as soon as no deformation could be detected under pressure.

## RESULTS AND DISCUSSION

**Synthesis and Appearance of Melting Gels.** A one-step acid-catalyzed method was employed to synthesize melting gels using 1-naphthyl, 2-naphthyl, and 9-phenanthrenyltrimethoxysilane (Figure 1). Liquid aryltrialkoxysilanes initially form a biphasic mixture with aqueous acid, which homogenizes through partial hydrolysis and condensation, producing methanol as a byproduct. Homogenization of PhSi(OCH<sub>3</sub>)<sub>3</sub> as monomer was reported to occur after approximately 6 min,<sup>27</sup> while 1-naphthyl- and 2-naphthyltrimethoxysilane investigated in this study required significantly more time to exhibit a visible reaction. The 1-NpSi(OCH<sub>3</sub>)<sub>3</sub> initially showed turbidity and yielded a clear liquid after about 4–6 h (the exact time is highly dependent on stirring speed and the size of the reaction vessel). In contrast, 2-NpSi(OCH<sub>3</sub>)<sub>3</sub> precipitated a white solid within the first 2 h, becoming homogeneous after about 6–24 h. The white solid could be isolated, and 2-NpSi(OH)<sub>3</sub> was identified as an intermediate in the reaction (Figures S4–S6). Contrary 1-NpSi(OCH<sub>3</sub>)<sub>3</sub> formed no stable, isolable silanol, suggesting that it immediately condenses after hydrolysis.

After gelation and drying at 110 °C for 24 h, both naphthyl-containing samples resulted in glass-like, hard, and transparent materials, which exhibited viscous flow at 110 °C (Figure 2). Lenses prepared with a thickness of 1.6 mm showed transmission of 86% and 88% at 450 nm (Figure S7) and a high refractive index of 1.6152 and 1.6096 at 589 nm for 1-NpMG and 2-NpMG (Figure S8), respectively, due to the

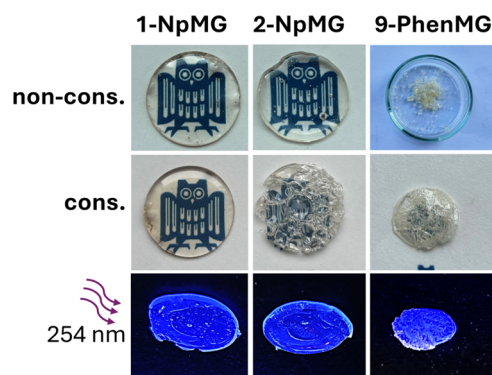


**Figure 2.** Images of non-consolidated and consolidated 1-NpMG, 2-NpMG, and 9-PhenMG under daylight and UV light (254 nm).

large number of delocalized  $\pi$ -electrons and the high polarizability of the naphthyl groups.<sup>26,36,39</sup>

In contrast to the naphthylalkoxysilanes, the 9-phenanthrenyltrimethoxysilane is solid and was therefore dissolved in acetone as the solvent is known to successfully lead to hydrolysis of 9-phenanthrenyltriethoxysilane.<sup>38</sup> Under the standard conditions (1.5 equiv of H<sub>2</sub>O, pH 2.5), no reaction of the monomer could be detected. Only by doubling the amount of water, a yellowish, hard, and brittle material was formed, indicating a successful polycondensation reaction. Softening at 110 °C could not be detected visually. As the temperature increased further, a slight flow of the resulting solid could be observed. The increase in the size of the aromatic system and the associated higher polarizability of the electrons resulted in a higher refractive index of 1.6476.

The known phenyl-containing melting gels exhibit not only thermoplastic properties at 110 °C but also thermoset behavior when treated at temperatures >130 °C. For this reason, all arylsilsesquioxanes produced were treated thermally at 200 °C for 24 h in order to induce further condensation reactions and further cross-linking. All materials exhibited a distinct yellow coloration [1-NpMG lenses showed a decrease in transmission to 64% at 450 nm (Figure S7)] after the temperature treatment.

Permanent hardening was observed in the 2-NpMG after 24 h when it was reheated to 200 °C. The absence of reflow properties was confirmed by bubbles remaining on the surface of the material, which were formed by the degassing of the byproducts, water and methanol (Figure 2). The material was also found to be insoluble in conventional solvents after curing, suggesting the formation of a macroscopic silica network.<sup>40</sup> The 9-PhenMG underwent permanent curing after the additional thermal treatment, but it remained soluble in conventional solvents, unlike the 2-NpMG. The 1-NpMG, on the other hand, remained soluble and remeltable, showing resistance to thermally induced curing. Although not all samples are cured completely, they are labeled as consolidated (cons.) in the following to illustrate a similar thermal treatment to the phenyl melting gel.

The different reactivities during the synthesis as well as the varying softening and curing behaviors demonstrate that the size and the isomerism of the organic group have a crucial influence on the structure and properties of polysilsesquioxanes. The different characteristics of the produced melting gels will be investigated in the following by using spectroscopic and thermogravimetric methods as well as SEC, MALDI-ToF mass spectrometry, and XRD.

**Analysis of Melting Gel Softening via Glass Transition Determination.** The glass-like behavior of both NpMGs and 9-PhenMG in the consolidated and non-consolidated states was analyzed using DSC. The phenyl melting gel, used as a comparison, exhibited a  $T_g$  of about 60 °C. This temperature remained constant across several heating cycles up to 110 °C, highlighting its reversible softening behavior within this range.<sup>27</sup> After consolidation, the  $T_g$  was no longer detectable, suggesting the formation of a three-dimensional network and the loss of reflow behavior.<sup>8</sup>

The  $T_g$  is directly related to the mobility of the polymer chains, which is influenced by factors such as cross-linking, the presence of hydroxy groups, and the nature of organic substituents.<sup>41–43</sup> As a result,  $T_g$  serves as an important indicator for assessing changes in the degree of cross-linking due to temperature-induced condensation reactions. The 1- and 2-naphthyl melting gels exhibit a  $T_g$  of around 50 and 40 °C, respectively (Figure 3), while the 9-PhenMG shows a

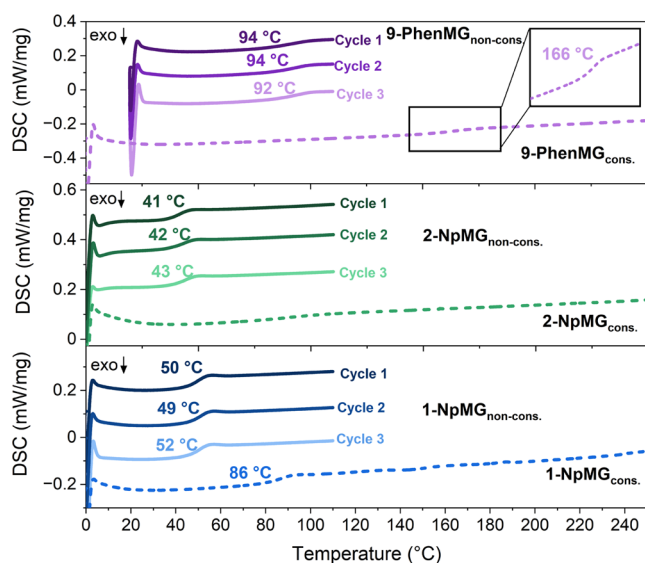


**Figure 3.** DSC measurement of non-consolidated and consolidated 1-Np-, 2-Np-, and 9-PhenMG, including determination of the  $T_g$ . Testing the reversible softening of the non-consolidated samples over three cycles up to 110 °C and monitoring the softening behavior of the consolidated samples in the range of 0–250 °C.

significantly higher value of 94 °C. All non-consolidated materials maintained stable glass transition temperatures across multiple heating cycles up to 110 °C, indicating that no structural changes occurred during this thermal treatment. The observed shift in softening to higher temperatures with increasing steric demand of the aromatic groups can be attributed to a reduction in intersegmental free volume, which consequently decreases chain mobility.<sup>26,44</sup>

However, cross-linking density also plays a crucial role. Despite having the smallest aromatic group, PhMG exhibits a  $T_g$  value higher than that of both 1- and 2-NpMG, indicating lower chain mobility due to a denser network, as highlighted in the NMR analysis.

After thermal treatment at 200 °C, the  $T_g$  increases by approximately 30 °C for 1-NpMG and 70 °C for 9-PhenMG, reflecting enhanced cross-linking. However, a complete disappearance of  $T_g$  is not observed, suggesting the absence of a macroscopic network for both samples. In 1-NpMG, it is reflected by the retention of visible flow properties after

thermal treatment. 9-PhenMG shows no flow behavior despite the presence of a  $T_g$ , which is due to the larger conjugated system with increased  $\pi$ – $\pi$  interactions and greater steric hindrance, whereby the movement of the polymer chains can also be hindered above the  $T_g$ .

In contrast, 2-NpMG exhibits only a slight increase in heat flow without a defined glass transition point, suggesting the formation of a three-dimensional network similar to that of PhMG. This finding aligns with visual and tactile observations, indicating that 2-NpMG is fully thermally cured.

**Structural Characterization. NMR Spectroscopy.**  $^1\text{H}$  NMR spectroscopy was employed to identify the organic substituents and to quantify the remaining nonhydrolyzed methoxy (OMe) groups, providing insights into the hydrolysis tendency of the monomer. Integration of the OMe groups relative to the aryl groups revealed that nonhydrolyzed groups remained intact in both naphthyl gels (Figures S9 and S10). The hydrolysis tendency, compared to that of PhMG, can be described in the following order: Ph > 2-Np > 1-Np, with 10, 13, and 19% remaining OMe groups (Figure 4a). Subsequent treatment at 200 °C resulted in further reduction of alkoxy groups in the naphthyl melting gels by further hydrolysis or condensation between the methoxy and hydroxy groups, visible in  $^1\text{H}$  NMR and  $^{13}\text{C}$  cross-polarization magic-angle-spinning (CP-MAS) NMR spectra (Figures S11 and 4b).

In contrast, 9-PhenMG shows almost complete hydrolysis of all methoxy groups, along with residues of acetone (Figure 4b), which can be attributed to the altered reaction conditions (higher water content, reaction in solvent). Furthermore, free phenanthrene was found via  $^1\text{H}$  NMR, as evidenced by sharp peaks in the aromatic region between 8.8 and 7.0 ppm, which are unusual for condensed polysilsesquioxanes (Figures S12 and S13). Si–C bond cleavage is a known phenomenon in the polycondensation of organosilica hybrids, as reported in the literature. It has been observed during the thermal condensation of diarylsilanediods,<sup>35,45</sup> whereby the stability of silanols decreased with increasing size of the aromatic compound.<sup>46</sup> The catalyzing effect of acid or base supports the cleavage, leading to the conclusion that the low Si–Phen bond stability, the acidic environment, and the increased water content cause partial Si–C bond cleavage in 9-PhenMG.

To investigate the local silicon environment, solid-state and liquid  $^{29}\text{Si}$  NMR spectra were collected (Figure 4c,d). Since only organotrimethoxysilanes were involved, species with one direct silicon–carbon bond ( $T^m$ ) are expected. Depending on the cross-linking, the chemical shift decreases with each added O–Si segment, marked with a superscript ( $T^0$ ,  $T^1$ ,  $T^2$ ,  $T^3$ ).<sup>47</sup> None of the samples showed a  $T^0$  peak, indicating the complete conversion of the monomers. Instead,  $T^1$ ,  $T^2$ , and  $T^3$  units are visible in all precursor gels in varying intensities, confirming the successful condensation reaction and highlighting variations in cross-linking density among the samples. Due to the detected Si–C bond cleavage in both the non-consolidated and consolidated 9-PhenMG, quaternary silicon ( $Q^n$ ) is expected in addition to T species. However, no signal was observed in the typical  $Q^1$ – $Q^4$  range between 85 and 110 ppm,<sup>48</sup> in either liquid or solid-state NMR. This absence is attributed to a low signal-to-noise ratio combined with a low concentration of Q units.

Due to the high number of varying oligomers or polymers with different chemical environments, partially condensed silsesquioxanes often give broad, ill-defined peaks that extend over a wide ppm range.<sup>49</sup> For example, 1-NpMG shows

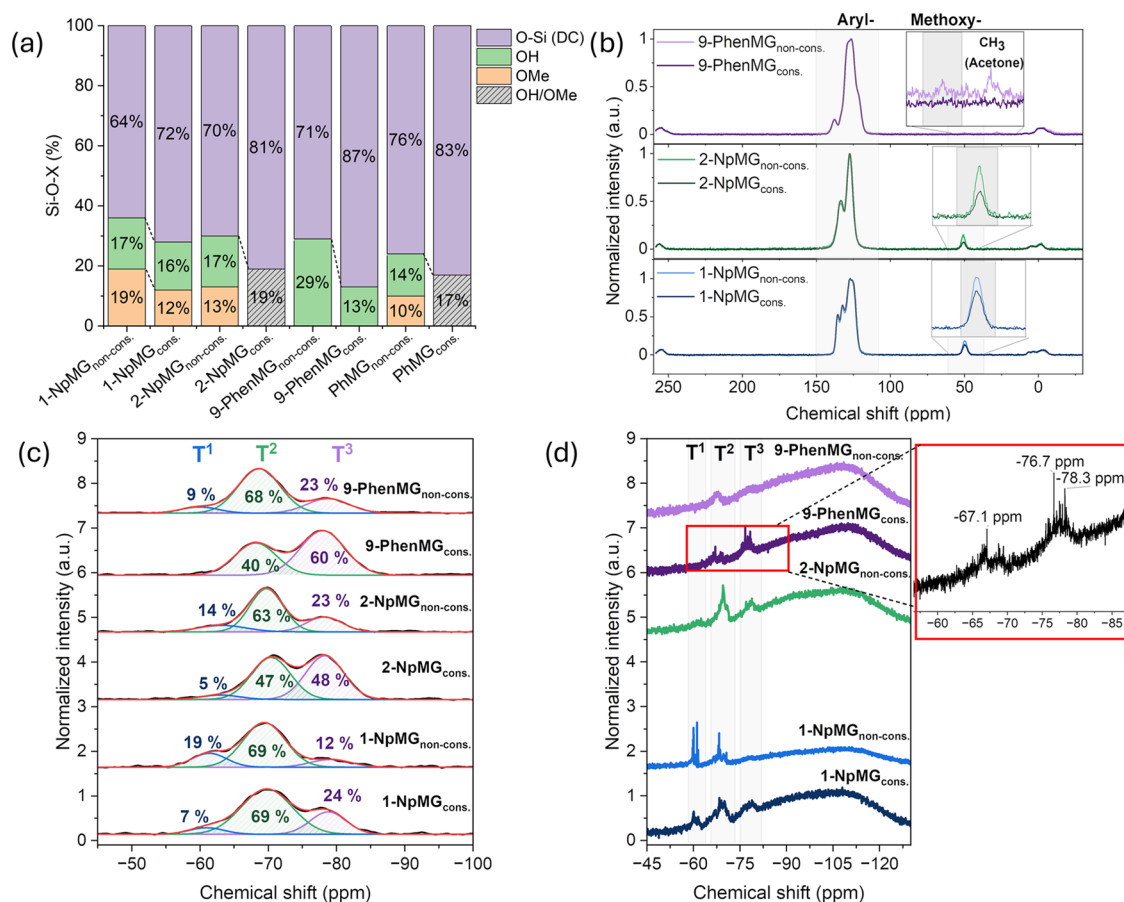


**Figure 4.** (a) Percentage of OH groups, OMe groups, and the degree of condensation (DC) of consolidated and non-consolidated 1-Np-, 2-Np-, 9-Phen-, and PhMG. PhMG values were taken from the literature.<sup>27</sup> The DC was calculated using deconvoluted <sup>29</sup>Si CP-MAS NMR according to the formula: DC (%) = (T<sup>3</sup> (%)·3 + T<sup>2</sup> (%)·2 + T<sup>1</sup> (%))/3. OH group percentages were derived from OMe group amounts, determined from <sup>1</sup>H NMR using the formula: OH (%) = 100 (%) – DC (%) – OMe (%), (b) <sup>13</sup>C CP-MAS NMR of consolidated and non-consolidated melting gels, with a zoom of the region of residual OMe groups, (c) <sup>29</sup>Si CP-MAS NMR of consolidated and non-consolidated melting gels, fitted with a Gaussian function, showing T<sup>1</sup>, T<sup>2</sup>, and T<sup>3</sup> percentages based on integral calculations, (d) liquid <sup>29</sup>Si NMR in CDCl<sub>3</sub> of consolidated and non-consolidated melting gels, with peak assignment for 9-PhenMG<sub>cons.</sub>.

individual peaks in the area of T<sup>1</sup> and T<sup>2</sup> before consolidation, indicating oligomeric units in an early stage of condensation (Figure 4d).<sup>50</sup> Thermal treatment, which increases cross-linking and molecular mass, results in peak broadening and an increase in T<sup>2</sup> and T<sup>3</sup>. 9-PhenMG, on the other hand, exhibits the opposite behavior. After consolidation, individual peaks appear in the T<sup>2</sup> and T<sup>3</sup> regions. This observation suggests that thermal treatment causes a reduction in the diversity of silsesquioxane species, leading to more ordered structures, such as cage-like forms.<sup>51</sup>

The amount of T<sup>n</sup> species and the degree of condensation can be determined semiquantitatively by deconvolution and integration of the <sup>29</sup>Si CP-MAS NMR spectra (Figure S14). Since cross-polarized measurements depend on both the distance and the amount of protons, the population of individual silicon species is often not accurately represented.<sup>52,53</sup> Given the large number of protons in the sample due to aryl groups, one can assume that the proton density is homogeneously distributed throughout the sample. This homogeneity minimizes errors in the relative quantification of the different T species and enables reliable trends in the degree of condensation to be observed [<sup>29</sup>Si SP-MAS and <sup>29</sup>Si CP-MAS NMR spectra for 2-NpMG<sub>cons.</sub> showed very similar spectra (Figure S15)].<sup>54</sup>

The degree of condensation (DC) shows the same tendency as the hydrolysis rate. With increasing steric demand of the organic group, the DC decreases in the order Ph > 2-Np > 1-Np (Figure 4a). Due to the changed reaction conditions, 9-PhenMG does not follow this trend and shows a similar DC to 2-NpMG with a value of 71%. After thermal treatment, all melting gels exhibit a significant increase in T<sup>3</sup> species and a decrease in T<sup>1</sup>, reflecting a marked increase in the number of cross-linked units. By subtracting the amount of bonded Si–O units (using DC value) and the amount of OMe groups obtained from the <sup>1</sup>H spectra, from the total amount of theoretically cross-linkable units, it becomes evident that OH groups remain in all samples, even after thermal treatment (Figure 4a). This persistence can be attributed to the aromatic groups, which sterically protect and hinder the remaining OH groups from participating in further thermally induced condensation reactions.

Overall, the NMR spectroscopic investigation demonstrates a significantly reduced hydrolysis and condensation tendency for 1-NpMG compared to 2-NpMG. Due to the same electronic situation, this behavior can be attributed to steric influences. Binding in the α-position results in a greater inhibition of attack by water or a Si–OH group compared to the β-position, resulting in a lower degree of condensation.

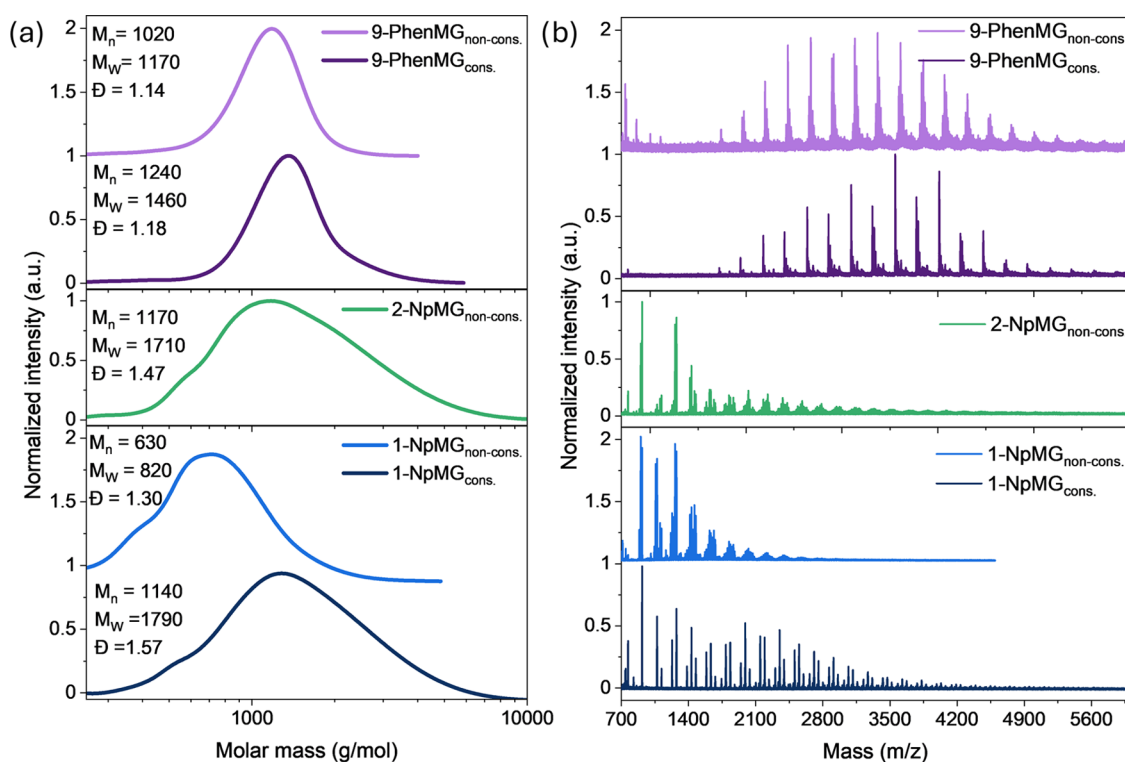


**Figure 5.** (a) SEC measurements (PS standard in THF) showing  $M_n$ ,  $M_w$ , and  $\bar{D}$ . (b) MALDI-ToF MS spectra of soluble consolidated and non-consolidated 1-Np-, 2-Np-, and 9-PhenMGs.

Despite thermal treatment, a large number of OH and methoxy groups remain stable, reflected in the retention of flow character and solubility of the 1-NpMG. The more extended 2-Np group containing molecule, which is more accessible for condensation reactions, leads to a higher degree of condensation after thermal treatment, making it more comparable with the DC of the known PhMG. In contrast, 9-PhenMG undergoes nearly complete hydrolysis of its methoxy groups due to the higher water content in the synthesis. The increased condensation tendency of the large amount of OH groups results in the highest cross-linking among all of the materials investigated. The fact that it is still soluble after consolidation as well as the formation of defined silsesquioxane species due to thermal treatment indicates mainly temperature-induced intramolecular condensation reactions.

**SEC/MALDI-ToF MS.** The NMR spectroscopy gives a good overview of hydrolysis and condensation tendencies, as well as the degree of cross-linking, but it does not provide information about the molecular mass of the silsesquioxane species formed. Hence, we applied SEC and MALDI-ToF MS to determine the molecular mass and polydispersity ( $\bar{D}$ ), as well as changes in molecular mass resulting from thermally initiated condensation reactions in all soluble samples (Figure 5). The non-consolidated 1-NpMG shows a low average molecular mass ( $M_w$ ) of 820 g/mol with a small  $\bar{D}$  value of 1.30 (Figure 5a), which corresponds well to the low DC and defined peaks detected via the NMR measurements. Thermal treatment at 200 °C results in an increase in size to  $M_w = 1800$  g/mol, along with a widening of the molar mass distribution, which is typical for intermolecular condensation reactions.<sup>21</sup> Nevertheless, the SEC results of the consolidated 1-NpMG remain low and are in a similar range to those of non-consolidated 2-NpMG, with a  $M_w = 1790$  g/mol and a polydispersity of 1.47. As the

molecular mass is an important parameter influencing flow behavior at temperatures above the  $T_g$ , the low  $M_w$ , even after thermal treatment, is visible in the lack of curing of the 1-NpMG.<sup>16</sup> Compared to the PhMG<sub>non-cons.</sub> with  $M_w = 3470$  g/mol and  $\bar{D} = 2.41$ ,<sup>27</sup> the measurements indicate a clear trend: the greater the steric hindrance (Ph < 2-Np < 1-Np), the lower the number and the weight-average molecular mass.

9-PhenMG differs from NpMGs in its low polydispersity of 1.14 and a molar mass that hardly changes during consolidation, indicating defined structural units and predominantly intramolecular condensation reactions.<sup>55</sup>

A more precise statement about the different silsesquioxane species formed and the type of condensation reaction can be made using MALDI-ToF MS. All melting gels give typical spectra characteristic of condensed polymers (Figure 5b).<sup>56</sup> Major clusters are identified and can be attributed to oligomers with a defined number of repeating units,  $n$  (Figure 6a,c). Within each  $n$ , the oligomers differ in the type and number of non-cross-linked units, forming minor clusters (Figure 6b,d). Replacing an OMe group with an OH group results in a reduction in a mass of 14 g/mol. The formation of a ring through the condensation of two OH groups or one OH and one OMe group results in mass losses of 18 and 32 g/mol, respectively. However, identifying the major clusters is challenging, particularly in naphthyl gels, as these span a wide mass range from the heaviest species (linear oligomers with only OMe groups) to the lightest species (fully cross-linked structures). Overall, the MALDI-ToF MS results align with the trend observed in SEC measurements, although the SEC results tend to slightly underestimate the mass of 9-PhenMG. This discrepancy can be attributed to the presence of the OH groups, which cause a more pronounced change in the hydrodynamic volume of 9-PhenMG compared to that of the polystyrene (PS) standards.

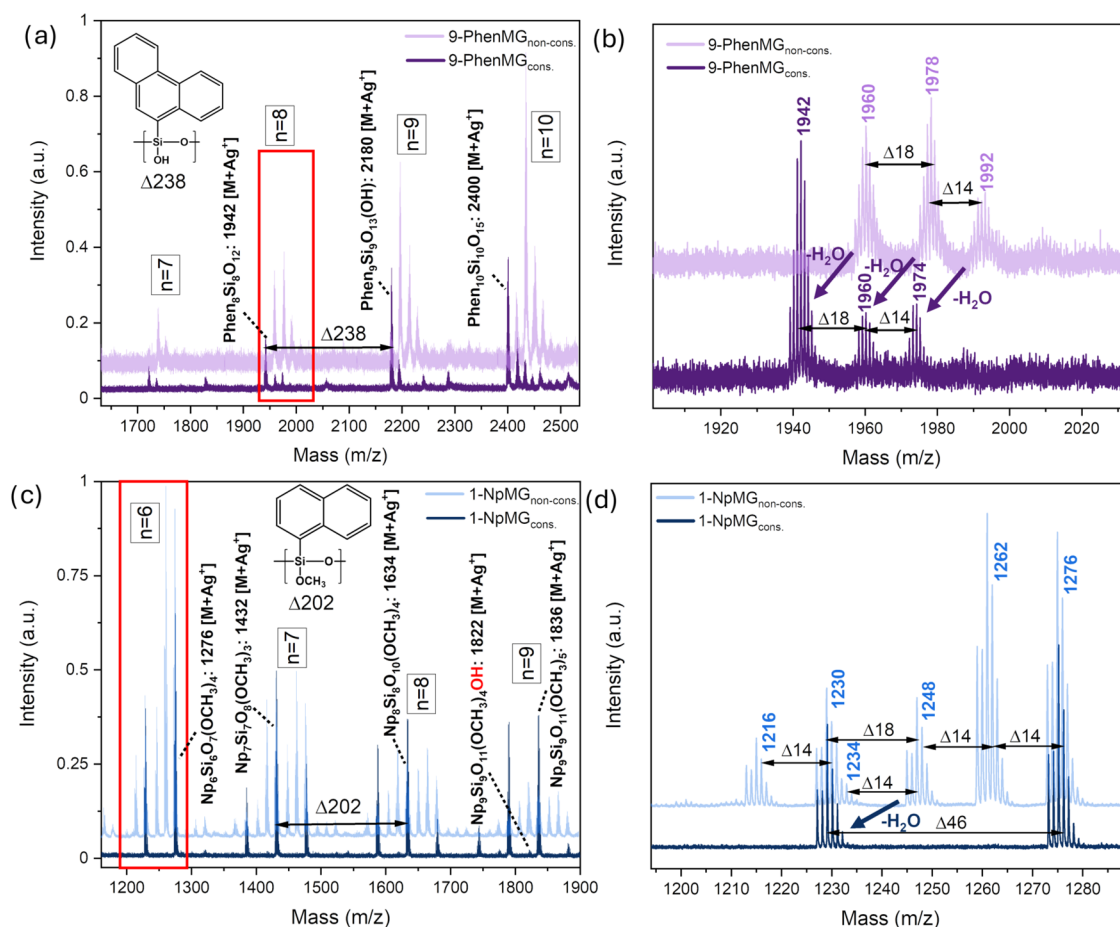


**Figure 6.** (a) Zoom in the full mass spectrum of the consolidated and non-consolidated 9-PhenMG, highlighting major clusters with 7–10 repeating units ( $n$ ) with a spacing between them of 238 u. The highest peak is assigned to the corresponding silsesquioxane unit of 9-PhenMG<sub>cons.</sub>, (b) single repeating unit with  $n = 8$  of the full mass spectrum of consolidated and non-consolidated 9-PhenMG. The distance between the peaks is 18 u for intramolecular condensation with the loss of water and 14 u for OH replacement by OMe, (c) zoom in the full mass spectrum of the consolidated and non-consolidated 1-NpMG, highlighting major clusters with 6–9 repeating units with a spacing between them of 202 u. The highest peak is assigned to the corresponding silsesquioxane unit of 1-NpMG<sub>cons.</sub>, (d) single repeating unit with  $n = 6$  of the full mass spectrum of consolidated and non-consolidated 1-NpMG. The distance between the peaks is 18 u for intramolecular condensation with the loss of water, 14 u for OH replacement by OMe, and 46 u for the replacement of two OMe groups by an Si–O bonding.

The comparison between the non-consolidated and consolidated samples is particularly insightful, as it provides information about inter- or intramolecular condensation reactions.

Due to its high degree of hydrolysis, 9-PhenMG shows well-separated major clusters with repeating units that differ in the number of rings and OH and OMe groups (Figure 6a). The comparison of the spectra between the non-consolidated and consolidated 9-PhenMG indicates that the thermally initiated condensation reactions are predominantly intramolecular. Looking at the main cluster with 8 repeating units in detail (Figure 6b), a mass reduction of 18 g/mol is observed, corresponding to the condensation of two OH groups and thus the formation of additional cycles, remaining  $T^8$  (1942 g/mol: Phen<sub>8</sub>Si<sub>8</sub>O<sub>12</sub> + Ag<sup>+</sup>) as the main peak as well as  $T^8$  with an open edge and OMe or OH groups (1960 g/mol: Phen<sub>8</sub>Si<sub>8</sub>O<sub>11</sub>(OH)<sub>2</sub> + Ag<sup>+</sup>, 1974 g/mol Phen<sub>8</sub>Si<sub>8</sub>O<sub>11</sub>(OH)(OCH<sub>3</sub>) + Ag<sup>+</sup>) as the second and third peaks. After consolidation,  $T^8$ – $T^{20}$  are detectable as the main peak, along with open variants containing stabilized hydroxy groups and a few remaining OMe groups. The well-defined peaks observed previously in the <sup>29</sup>Si NMR spectrum can thus be correlated

with one or more of these cubes. However, a precise assignment of these peaks is not possible without isolating the individual components. The overall mass spectrum shows no change in the number of repeating units due to the thermally initiated condensation reactions and only a reduction in the minor cluster, which highlights the intramolecular ring formation to highly cross-linked silsesquioxanes.<sup>57</sup>

In comparison, both naphthyl gels exhibit a significantly more complex mass spectrum. Due to a high number of hydroxy and methoxy groups, each major cluster consists of many minor clusters, differing by 14 g/mol, reflecting variations in the ratio of OH/OMe groups (Figure 6c). However, consideration of the overall spectrum of 1-NpMG<sub>cons.</sub> shows a clear shift toward higher molar masses after thermal treatment at 200 °C, resulting from intermolecular condensation reactions. A closer look at oligomers with  $n = 6$  (Figure 6d), for example, reveals partially cross-linked silsesquioxanes containing only methoxy groups after consolidation. Within individual clusters, the oligomers differ by a mass delta of 46 g/mol, which corresponds to the formation of a ring by the reduction of two OMe groups (1230 g/mol: 1-Np<sub>6</sub>Si<sub>6</sub>O<sub>8</sub>(OCH<sub>3</sub>)<sub>2</sub> + Ag<sup>+</sup> and 1276 g/mol: 1-

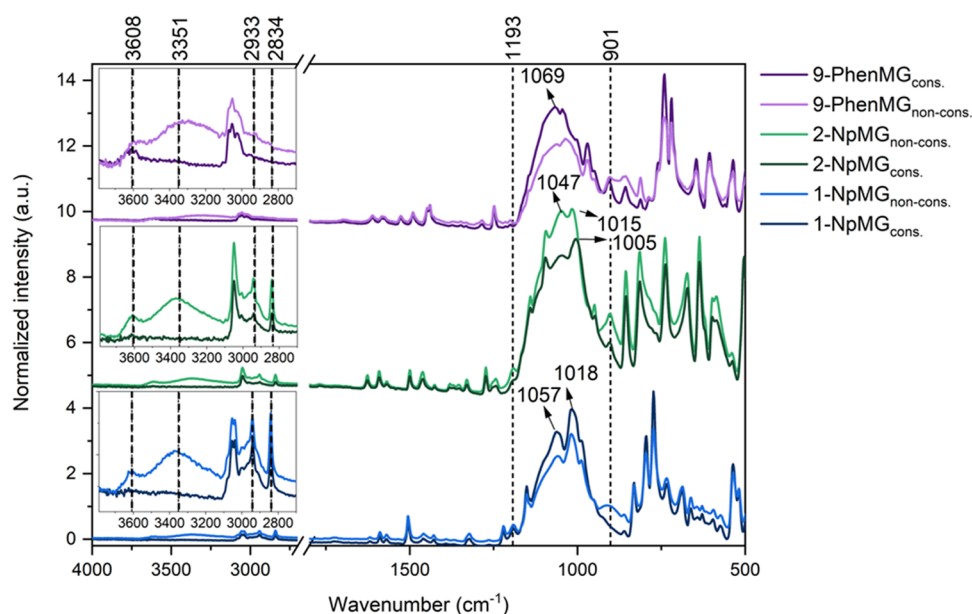


**Figure 7.** FTIR spectra of consolidated and non-consolidated 1-Np-, 2-Np-, and 9-PhenMGs with a zoomed view of the OH region and highlighting of key vibration peaks.

$\text{Np}_6\text{Si}_6\text{O}_7(\text{OCH}_3)_4 + \text{Ag}^+$ ). It can be assumed that the OH groups in the 1-NpMG are less stabilized, as oligomers with isolated hydroxyl groups are observed only from  $n = 9$ .

The microstructure of 2-NpMG<sub>non-cons.</sub> is comparable to that of 1-NpMG<sub>non-cons.</sub>, with the distinction that oligomers can be detected in higher mass ranges. As already recognized by the increased molar mass in the SEC measurements and the higher DC in the NMR measurements, the MALDI-ToF MS results confirm the formation of larger silsesquioxane units with an increased number of repeating units. Compared to 1-NpMG and 9-PhenMG, a further reduction in the stability of the OH groups is expected, promoting a stronger tendency toward intermolecular condensation and intermolecular entanglement.

The SEC/MALDI-ToF MS measurements highlight the influence of the aromatic groups on the molar mass, OH group stabilization, and type of condensation reaction. Depending on the size of the aryl group, either inter- or intramolecular condensation reactions are favored. Phenanthrenyl, the largest moiety investigated here, forms oligomers with a size of 7–20 repeating units. Thermally initiated condensation reactions occur intramolecularly within these oligomers, resulting in a significantly higher degree of cross-linking but minimal change in molecular size. The preferred formation of both open and closed cubes is observed. 1-NpMG with 1-naphthyl as the next largest organic group exhibits not only intramolecular but also intermolecular condensation reactions. This results in an increase in the average molecular mass and a broadened molar mass distribution. In contrast to 9-PhenMG, a large number of OMe groups are present, stabilizing the oligomers with a small number of repeating units. The presence of linear polysilsesquioxanes with a few rings or a ladder-like structure can be predicted. The 2-naphthyl group has the lowest steric hindrance due to its extended structure. This leads to an increased hydrolysis rate and a stronger condensation tendency, as evidenced by the significantly higher  $M_w$  compared to 1-NpMG<sub>non-cons.</sub>. It can be assumed that the consolidation promotes intermolecular condensation reactions, resulting in the formation of an extended network, which causes insolubility and a lack of chain mobility.

**ATR-FTIR Spectroscopy.** ATR-FTIR spectroscopy was used for further analysis of the silsesquioxane structure. The process of hydrolysis and condensation can be detected by examining specific vibrational bands of methoxy- and hydroxy groups.<sup>58</sup> All polysilsesquioxanes display a reduction in the signals from the OMe at 2834 and 2933  $\text{cm}^{-1}$  ( $\nu\text{CH}_3$ ), 1193  $\text{cm}^{-1}$  ( $\rho\text{CH}_3\text{O}$ ), and 1069  $\text{cm}^{-1}$  ( $\nu\text{CO}$ ) due to the hydrolysis reaction (Figure 7).<sup>59,60</sup> However, the complete disappearance of these absorption bands is not observed in 1- and 2-NpMG, demonstrating the persistence of OMe groups, consistent with results from NMR measurements. Furthermore, an absorption band corresponding to OH groups is visible at 900  $\text{cm}^{-1}$  and between 3000 and 3700  $\text{cm}^{-1}$ . A distinction can be made between OH groups interacting via hydrogen bonding (3000–3500  $\text{cm}^{-1}$ ) and isolated OH groups (>3600  $\text{cm}^{-1}$ ).<sup>8</sup> Upon thermal treatment at 200 °C, the associated OH groups nearly disappear. Hydroxy groups shielded by the aromatic moiety remain visible as isolated groups in the range >3600  $\text{cm}^{-1}$ .

Condensation reactions and resultant Si–O–Si cross-linking become apparent through absorption in the Si–O–Si vibration range between 1000 and 1150  $\text{cm}^{-1}$ . This segment of the spectrum is particularly interesting, as it provides insights into the forming silsesquioxane network.<sup>61,62</sup> Both NpMGs exhibit a defined Si–O–Si vibration band focused on lower wavenumbers between 1000 and 1100  $\text{cm}^{-1}$  with two maxima around 1040–1060  $\text{cm}^{-1}$ , featuring the Si–O–Si network with low symmetric linear or cross-linked units, and 1015/1018  $\text{cm}^{-1}$  representing strained cycles.<sup>63–65</sup>

With consolidation, only a definition of the existing peaks is observed in 1-NpMG, indicating no major change in the microstructure despite further condensation reactions.

In contrast, the FTIR spectra of 2-NpMG<sub>cons.</sub> show a decrease in the Si–O–Si network band at 1058  $\text{cm}^{-1}$ , while the band corresponding to the strained cycles shifts from 1018 to 1005  $\text{cm}^{-1}$  and becomes dominant. The formation of a band in the low wavenumber range of the Si–O–Si region is also reported in the literature after the thermal condensation of silanols, such as  $\text{PhSi}(\text{OH})_3$ .<sup>66,67</sup> During the melting gel synthesis, the partial formation of 2-NpSi(OH)<sub>3</sub> was detected.

It can be assumed that the solvent-free, thermal condensation of silanols preferentially results in the formation of cyclic structures (like  $(\text{Si}-\text{O})_6$  or cyclotrisiloxanes).<sup>68</sup> The absence of softening and the lack of solubility indicate that these cyclic structures are condensed, forming a dense network.

The Si–O–Si region of 9-PhenMG has no prominent peaks and is more concentrated around  $1070\text{ cm}^{-1}$ , representing open cages of varying sizes, as detected in the MALDI-ToF MS.<sup>69</sup> Further intramolecular condensation reactions lead to the formation of more defined silsesquioxanes, including fully cross-linked cages. This transformation is visible in the spectrum by a narrowing of the full width at half-maximum in the Si–O–Si region.

Variances in the structure of the melting gels, influenced by the different organic groups, were detected via MALDI-ToF and manifested in the Si–O–Si vibration range. In 1-NpMG, small low-symmetry silsesquioxane structures, such as small rings, linear chains, or ladders, are found, while the 2-Np substituent appears to favor condensed cycles, as 2-naphthyltrihydroxysilane is formed as an intermediate during synthesis, dictating subsequent structure development. In contrast, cage structures of different sizes are observed in 9-PhenMG, represented by a broad band around  $1070\text{ cm}^{-1}$ . All samples show a definition of the FTIR region after thermal condensation, indicating the formation of a more ordered silsesquioxane structure.

**Powder XRD.** PXRD measurements are a known method to study the structural order of polysilsesquioxanes. Ladder-like polysilsesquioxanes or layered polysiloxanes typically exhibit two broad, amorphous reflections in the diffractogram. The assignment of the first reflection ( $d_1$ ) varies in the literature, attributed to the width of ladder-like structures<sup>70–72</sup> or interpreted as the intermolecular chain-to-chain distance in ladders or between layers or cages.<sup>51,73,74</sup> In both interpretations, the position of the first signal depends on the type of the organic group and the defect concentration. Bulkier and more spatially extended organic groups lead to greater separation between silsesquioxane layers, resulting in a higher  $d_1$  value and lower packing density.<sup>3</sup> Defects, such as non-condensed methoxy or hydroxy groups, as well as changes in the conformation of the organic group, lead to a lower  $d_1$  distance and a decrease in the relative intensity of the first reflection compared to the second ( $R$  value).<sup>72,75</sup> All three aryl melting gels display a signal corresponding to  $d_1$  (Figure 8), indicating a layered structure. The low  $R$  value (Table 1) and broadening of the first reflection suggest a low long-range order and a structure that is rich in defects. The  $d_1$  value of the non-consolidated gels represents the increased bulkiness and spatially extended length in the order Ph < 1-Np < 2-Np < 9-Phen, as well as the chain packing density in reverse order. Temperature-induced cross-linking becomes evident by an increase in the  $d_1$  values, accompanied by an increase in the  $R$  value. NMR and MALDI-ToF MS results indicate still a defect-rich structure with non-condensed groups, even in the consolidated materials. Therefore, observed  $d_1$  values are far from an ideal ordered arrangement and could potentially be significantly larger.

The  $R$  value increases in the order 1-Np < 2-Np < Ph < 9-Phen. The increase in order can be correlated with the proportion of hydrolyzed species detected by NMR spectroscopy. It has been shown that silanols thermally condense, thereby retaining the structure that predominates in the crystal.<sup>35</sup> The higher the proportion of OH groups, the more

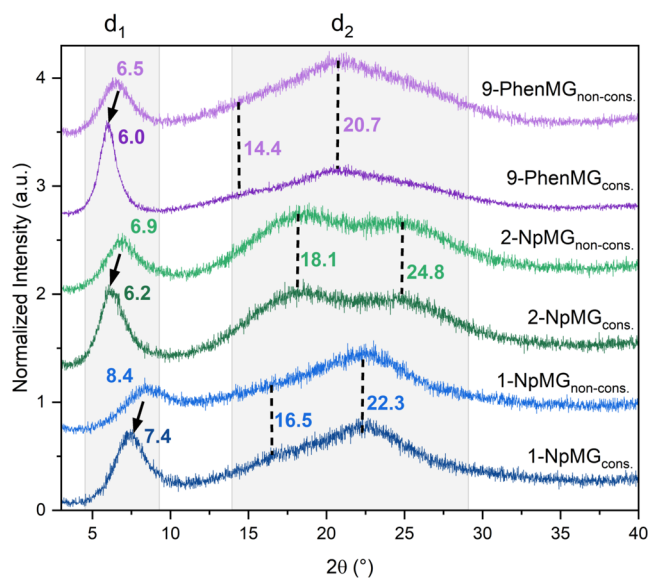


**Figure 8.** PXRD patterns of consolidated and non-consolidated 1-Np-, 2-Np-, and 9-PhenMG with marked positions of the  $d_1$  and  $d_2$  reflections.

**Table 1.**  $d_1$ ,  $d_2$ , and  $R$  Values of Consolidated and Non-consolidated 1-Np-, 2-Np-, and 9-PhenMG Measured by PXRD<sup>a27</sup>

sample		maximum $d_1$ [nm]	maximum $d_2$ [nm]	$R$ ( $I(d_1)/I(d_2)$ )
1-NpMG	non-cons.	1.05	0.40	0.62
	cons.	1.19		0.90
2-NpMG	non-cons.	1.28	0.49	0.71
	cons.	1.42		1.01
9-PhenMG	non-cons.	1.36	0.43	0.78
	cons.	1.47		1.78
PhMG	non-cons.	0.83	0.45	0.98
	cons.	0.98		1.15

<sup>a</sup>Values for PhMG were taken from the literature.<sup>27</sup>

structuring units are present, resulting in a more uniform structure.

The amorphous part of the material is represented by a  $d_2$ . The phenyl melting gel shows an amorphous, broad signal at 0.45 nm, consistent with the literature attributing this to the average thickness of the molecular chains.<sup>3,72,76</sup> The value is described as independent of the organic group and the cross-linking. Unexpectedly, all melting gels exhibit two overlapping diffuse peaks in the range of  $d_2$ . The 2-NpMG display two distinct maxima at 0.49 and 0.36 nm, while 1-NpMG and 9-PhenMG show a maximum at 0.40/0.43 nm with a shoulder at 0.54/0.61 nm. As the consolidation leaves the reflections unchanged, but structural change becomes apparent via IR and NMR, it can be assumed that the position of  $d_2$  is not directly linked to the resulting structural arrangement. The observed differences are likely influenced by the asymmetric nature of the organic group in comparison with the phenyl substituent.

XRD measurements confirm the presence of a layered structure in all of the melting gels. However, the low  $R$  value indicates a high degree of structural disorder in the non-consolidated materials due to a large amount of non-condensed hydroxy and methoxy groups. The size of the organic substituent is reflected in the  $d_1$  parameter, which

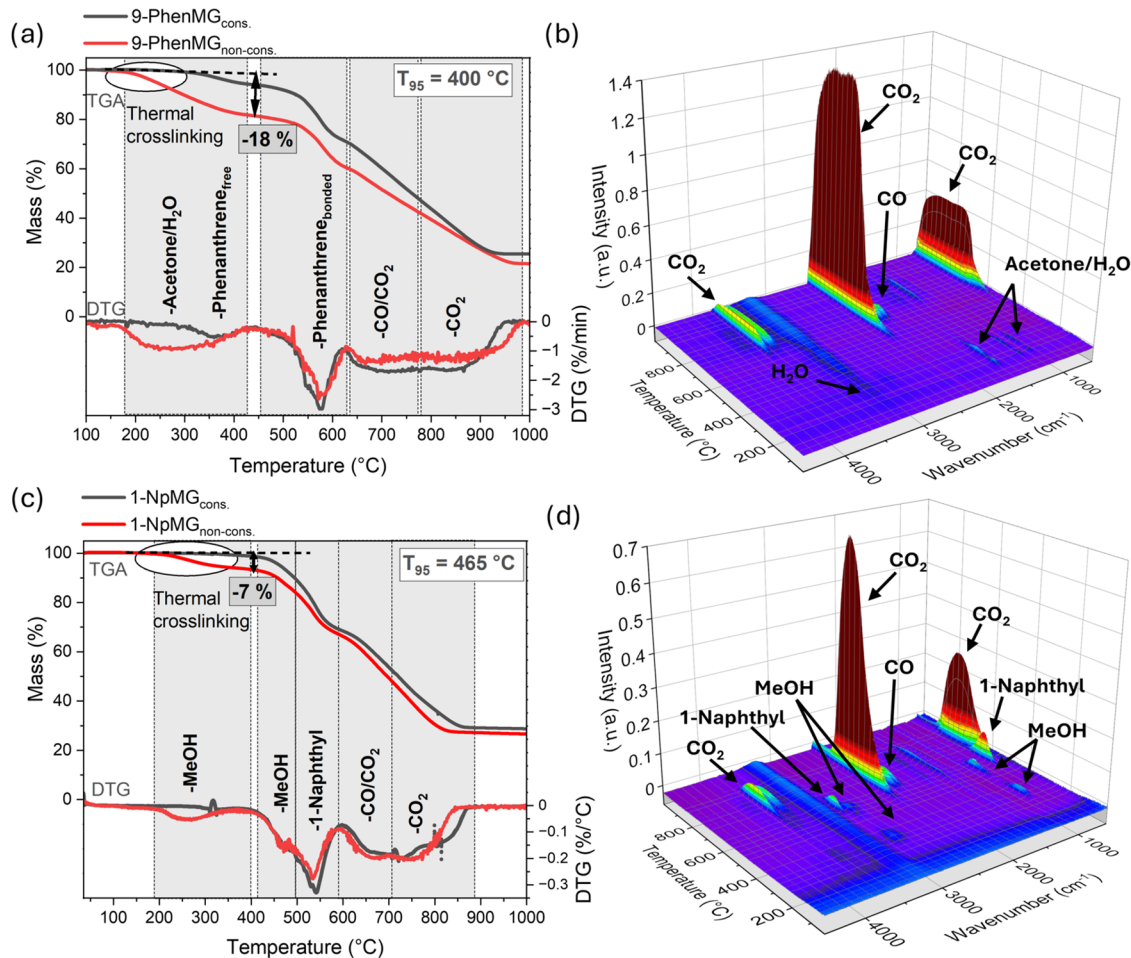


**Figure 9.** TG curve under air and DTG curve of the consolidated and non-consolidated melting gels, with assignment of the gases released during each decomposition stage,  $T_{95}$  value of the consolidated melting gel, and the marked mass loss in the first decomposition stage of the non-consolidated melting gel: (a) 1-NpMG and (c) 9-PhenMG. Three-dimensional (3D) graphic of the FTIR spectra of degradation products as a function of temperature, with the assignment of the detected gases: (b) 1-NpMG<sub>non-cons.</sub> and (d) 9-PhenMG<sub>non-cons.</sub>

correlates with the interlayer distance and increases from phenyl to phenanthrenyl. Thermal treatment and further cross-linking lead to structural expansion and increased ordering, consistent with FTIR results. The quantity of OH groups acting as structuring elements proves to be a crucial factor in thermally initiated condensation.

**Thermal Analysis.** TGA/Thermogravimetric Analysis-Fourier Transform Infrared Spectroscopy (TG-FTIR). Polysilsesquioxanes are known for their exceptionally high thermal stability, which is attributed to their high Si–O binding energy.<sup>77</sup> In addition, the cross-linking properties minimize bond cleavage and ring formation, which occurs more frequently in linear polysiloxanes during thermal decomposition.<sup>78,79</sup> The organic group also plays an important role in decomposition. Phenyl groups have been found to be particularly stable, both in an inert atmosphere and under air.<sup>80</sup> The phenyl melting gel showed a mass loss of 5% ( $T_{95}$  value) in an oxygen atmosphere at 400 °C in its non-consolidated state and at 510 °C after the consolidation, demonstrating a high thermal stability, which is typical for polyphenylsilsesquioxanes.<sup>27</sup> By using TG-FTIR, a 3.95% mass loss due to water and methanol was detected starting at 200 °C, which resulted from the thermally induced condensation reactions. Further decomposition, involving Si-Ph bond cleavage, proton abstraction, and oxidation of free carbon,

was observed at 590 and 670 °C through the monitoring of benzene, CO<sub>2</sub>, and CO.

The influence of the different polycyclic aromatic groups on thermal stability and decomposition under air was investigated via TGA and TGA-FTIR, analogous to the studies on PhMG. The decomposition of naphthyl and phenanthrenyl melting gels is very similar to that of the polyphenylsilsesquioxane. All samples show three defined mass losses in the range 180–380 °C; 400–650 °C; and 600–950 °C, whereby the derivative thermogravimetric (DTG) curves indicate overlapping decomposition stages in the range of the second and third mass losses for NpMGs (Figures 9a,c and S16). For the qualification of the gases produced during consolidation and further decomposition, TG-FTIR measurements were performed (Figures 9b,d and S16).

The first mass loss, starting at about 200 °C for the NpMGs, can be assigned to the reaction of OMe and OH groups, primarily forming methanol as byproduct. Water cannot be detected in the FTIR spectra of the gaseous decomposition products, possibly due to a further hydrolysis reaction of the remaining methoxy groups. After consolidation, the initial mass loss is no longer visible, and further decomposition of the materials does not start until 400 °C. This is explained by the condensation of all available and interacting OH groups, and only the addition of external agents (for example, a base as a

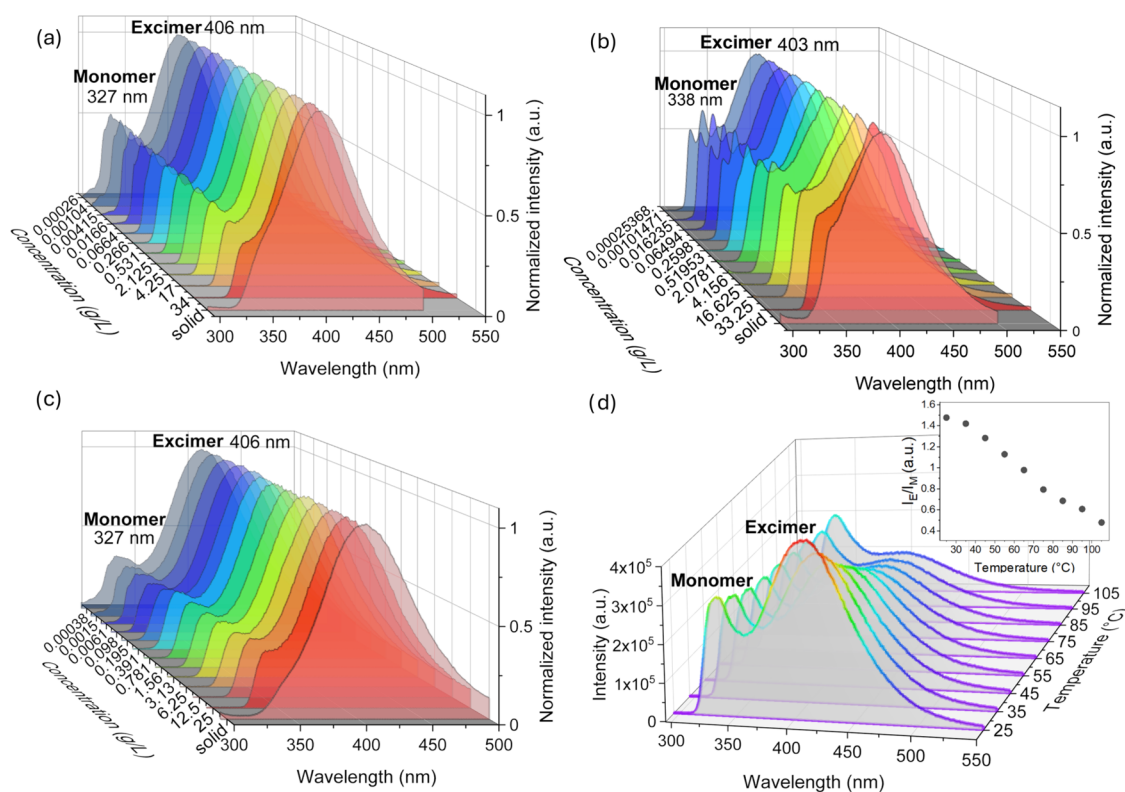


**Figure 10.** Concentration-dependent fluorescence spectra of (a) 1-NpMG<sub>non-cons.</sub>, (b) 2-NpMG<sub>non-cons.</sub>, and (c) 1-NpMG<sub>cons.</sub> in DCM with  $\lambda_{\text{ex}} = 285$  nm. (d) Temperature-dependent measurements of 1-NpMG<sub>non-cons.</sub> in dimethyl sulfoxide (DMSO) between 25 and 105 °C,  $\lambda_{\text{ex}} = 285$  nm,  $c = 0.6$  g/L. The inset shows the temperature-dependency excimer-to-monomer fluorescence ratio.

catalyst) would enable further cross-linking in the cured materials. The two naphthyl groups primarily differ in the magnitude of the first step, with the 1-NpMG exhibiting a mass loss of about 1.5 times larger than that of the 2-NpMG. This difference can be explained by the lower DC of the non-consolidated 1-NpMG and an increasing number of condensation reactions, resulting in a higher loss of byproducts. However, both materials show high thermal stability, with a  $T_{95}$  of about 460 °C after temperature treatment.

The 9-PhenMG exhibits a significantly larger first degradation step of about 18%, starting earlier at 180 °C (Figure 9c). Analysis of the gaseous components reveals the presence of mainly residual solvent from the synthesis and water from condensation reactions (Figure S17). The removal of acetone at such a late stage suggests interactions between the carbonyl group and the silanols of the melting gel via hydrogen bonds.<sup>81</sup> However, the 18% mass loss cannot be attributed solely to the condensation byproducts and residual solvents. It is to be expected that the sublimation of free phenanthrene, detected by <sup>1</sup>H NMR, is also reflected in this stage. Since no condensation stage occurs in the consolidated material, the mass loss of around 350 °C relates to the release of the aromatic compound. Due to the high boiling point of phenanthrene, it crystallizes in the transfer line before reaching the IR detector and is therefore not visible in the IR spectra of the gaseous degradation products (<sup>1</sup>H NMR spectrum of the crystals from the TGA furnace is given in Figure S18).

The second mass loss begins around 400 °C. Methanol is initially detected during this stage in the naphthyl melting gels, coming from the decomposition of OMe groups that were not reacted in the first condensation step. Overlapping with the formation of methanol, the FTIR spectrum shows an

absorption of the aromatic C–H vibration. It indicates the cleavage of the Si-naphthyl bond and the detection of naphthalene.<sup>79</sup> The 9-PhenMG shows a mass loss at a similar temperature, which cannot be detected by FTIR. The cleavage of the Si-phenanthrenyl bond and the loss of the aromatic group are expected in this step, similar to those of the NpMGs.

Complete oxidation of the carbon results in a release of CO and CO<sub>2</sub> during the final degradation step, visible in all three silsesquioxanes between 600 and 950 °C.<sup>82</sup>

The different attachment of the naphthyl group and the size of the aromatic group do not appear to have a significant effect on thermal stability and oxidative decomposition. All materials reveal a thermal stability of  $\geq 400$  °C, with their thermal decomposition differing primarily in the number of remaining hydroxy and methoxy groups. The high thermal oxidative stability distinguishes the aromatic melting gels from the reversibly softenable silsesquioxanes with alkyl groups or alkyl spacer between the silicon and the aromatic group, as described in the literature.<sup>28,33,83</sup> Since 9-PhenMG contains only a very small number of OMe groups, no release of methanol can be identified. However, acetone, interacting via hydrogen bonds, and phenanthrene, cleaved by acidic polycondensation during the synthesis, can be detected. The 1-Np- and 2-NpMG differ only in the size of the condensation step, which is dependent on their degree of condensation.<sup>28,83</sup>

**Fluorescence Analysis.** Under UV light, the aromatic melting gels show pronounced fluorescence behavior (Figure 2). Fluorescence spectroscopy can be used to investigate interactions within polymers, as fluorescence is highly dependent on the environment of fluorophores. Polycyclic aromatic hydrocarbons such as pyrene, benzene, naphthalene, perylene, and their derivatives are known to show a

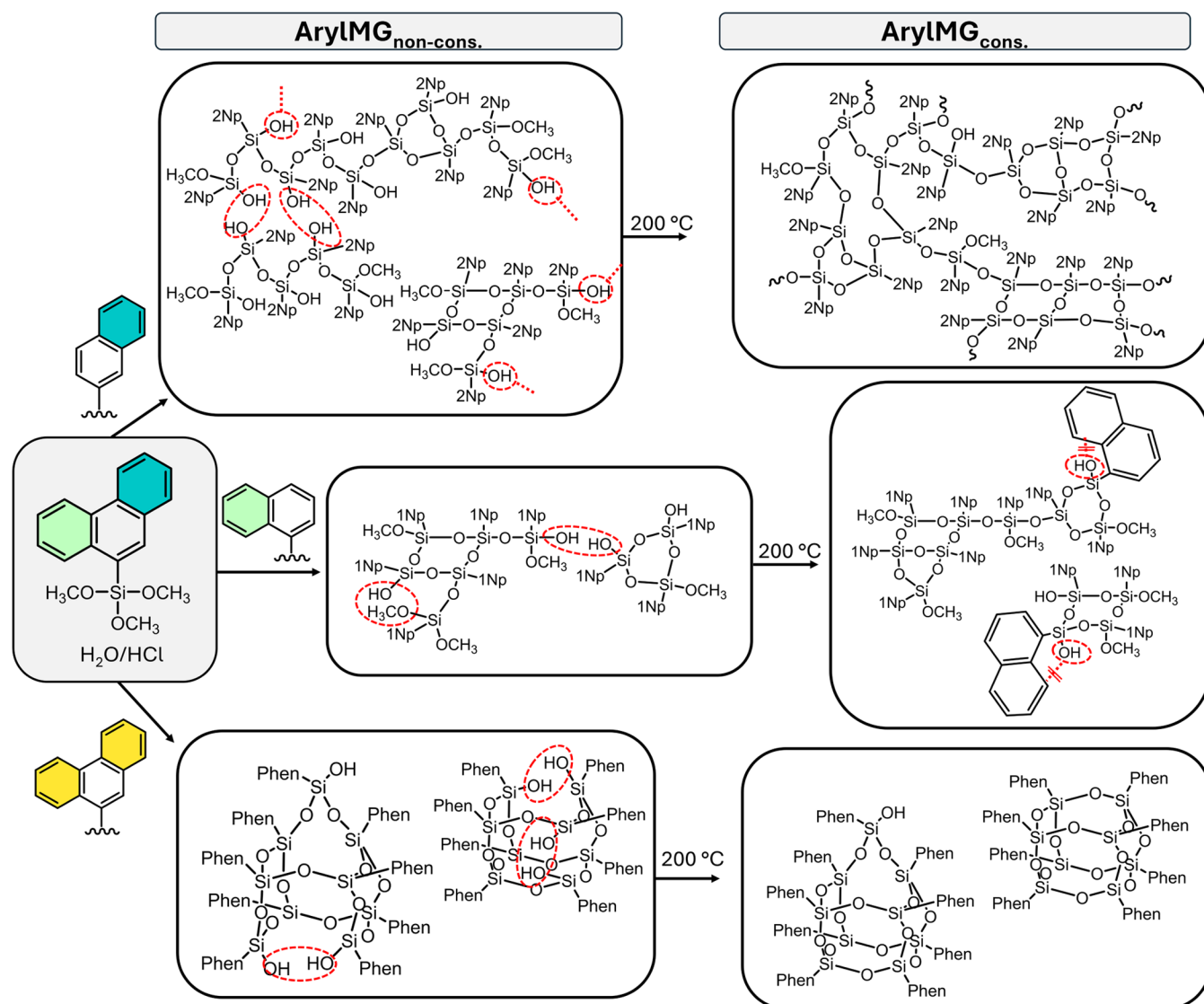


**Figure 11.** Schematic representation of the proposed structures of the three investigated melting gels (1-NpMG, 9-PhenMG, and 1-NapMG) in their non-consolidated and consolidated forms. The structural motifs shown are a representative selection of the units postulated in the materials and reflect the most important characteristics of the respective material state.

concentration-dependent formation of a structureless band. This band is attributed to excimers, which result from an attachment of an excited aromatic molecule with an unexcited one.<sup>84–86</sup> Excimer formation can also occur within oligomers and polymers, such as polystyrenes,<sup>87</sup> polyvinyl naphthalenes,<sup>88</sup> and even polyphenylsiloxanes<sup>89</sup> or polyphenylsilsequioxanes,<sup>90</sup> provided the aromatic groups adopt a stable sandwich conformation.<sup>91</sup> Concentration-dependent measurements allow one to distinguish between inter- and intramolecular excimer formation. If the ratio between the monomer and excimer band in a diluted solution shows no concentration dependence, interactions within the polymer chain can be expected.<sup>90</sup> As PhMG is known to form inter- and intramolecular excited dimers,<sup>27</sup> concentration-dependent fluorescence spectra were also measured for the soluble naphthyl- and phenanthrenyl melting gels in the consolidated and non-consolidated states.

Naphthalene shows a moderately prominent excimer band at high concentrations at room temperature, which becomes more prominent in certain naphthalene derivatives, with a

maximum between 392 and 408 nm.<sup>92</sup> Concentration-dependent fluorescence spectra of the monomers 1-Np- and 2-NpSi(OMe)<sub>3</sub> in DCM confirm this observation (Figures S19 and S20, absorption spectra in DCM of monomers and polymers see Figure S21). 1-NpSi(OMe)<sub>3</sub> shows monomer fluorescence at 329 nm with shoulders at 323 and 335 nm, while 2-NpSi(OMe)<sub>3</sub> presents three defined peaks at 323, 338, and 353 nm. A red shift is observed due to self-absorption at high concentrations. In the absence of solvent, a structureless band at 403 nm (1-NpSi(OMe)<sub>3</sub>), as well as a structureless band at 390 nm (2-NpSi(OMe)<sub>3</sub>), dominates the spectra, which can be assigned to the excimer band. The ratio between monomer and excimer fluorescence is strongly concentration-dependent, which is typical for intermolecular excimer fluorescence. In contrast, phenanthrene is known not to exhibit excimer fluorescence, except under exceptional environments or the use of substituted phenanthrenes.<sup>93–95</sup> This behavior is mirrored in the monomer 9-PhenSi(OMe)<sub>3</sub>, which displays a defined monomer fluorescence with a peak maximum at 367 nm, accompanied by a spectral shift caused

by self-quenching at increased concentrations (Figure S22).<sup>96</sup> Unlike the naphthyl monomers, 9-PhenSi(OMe)<sub>3</sub> does not show a red-shifted, unstructured band, indicating the absence of excimer formation.

The non-consolidated melting gels containing naphthyl groups show the previously described peaks corresponding to excimer and monomer fluorescence (Figure 10a,b). The excimer band, which appears at 406 nm for 1-NpMG and at 403 nm for 2-NpMG, persists even at low concentrations <0.0026 g/L. As soon as the spectrum is no longer influenced by self-absorption, the ratio of monomer to excimer fluorescence remains constant. At this point, the oligomeric structures are fully separated by solvent, eliminating intermolecular interactions. The fluorescence detected under these conditions can be assigned to intramolecular excimer fluorescence, which suggests that the naphthyl groups, both in  $\alpha$  and  $\beta$  positions, must be present in a symmetrical sandwich conformation. The same experiments were repeated with consolidated, soluble 1-NpMG (Figure 10c). A prominent, concentration-independent excimer band is also formed at 406 nm. Compared to the non-consolidated gel, the ratio of excimer to monomer fluorescence increases from  $I_{\text{Ex}}/I_{\text{M}} = 1.9$  for the non-consolidated to  $I_{\text{Ex}}/I_{\text{M}} = 3.2$  for the consolidated sample. It can be concluded that the additional cross-linking leads to an increased number of intramolecular excimers, suggesting a more ordered system with a lower number of defects.<sup>97</sup> These findings align with the XRD measurements, which also demonstrated structural ordering induced by the thermal treatment.

In contrast, 9-PhenMG exhibits no excimer band in either the non-consolidated or consolidated state (Figure S23), consistent with the known behavior of phenanthrenyl substituents, which do not form excimers.

The effect of temperature on excimer formation in 1-Np- and 2-NpMG was studied in DMSO over a range of 25–105 °C. In both melting gels, the excimer fluorescence decreases with increasing temperature, while the monomer fluorescence remains largely unaffected, leading to a reduction in the relative ratio  $I_{\text{Ex}}/I_{\text{Em}}$  (Figures 10d and S24). The temperature dependence of the excimers is a known phenomenon in the literature and can be attributed to thermal dissociation.<sup>98,99</sup> These findings highlight the thermally initiated changes in aromatic interactions that contribute to the observed thermo-plastic behavior.

## CONCLUSIONS

In this study, we investigated the influence of the aromatic group size and isomerism on the structural and thermal properties of polysilsesquioxane-based melting gels. Through acid-catalyzed polycondensation, we synthesized polysilsesquioxanes from 1-naphthyl, 2-naphthyl, and 9-phenanthrenyl-trimethoxysilanes, examining their behavior in terms of reversible softening at 110 °C and irreversible curing at 200 °C, similar to known phenyl-containing melting gels.

Our structural analyses revealed that aryl group isomerism and size significantly affect molecular mass, cross-linking density, and overall structure (Figure 11). 1-NpMG forms low-mass oligomers with numerous stabilized non-cross-linked OH and OMe groups. The low degree of condensation allows reversible softening and solubility even after thermal treatment at 200 °C, making the material resistant to thermal curing. In contrast, the more linear and less bulky structure of the 2-naphthyl group facilitates cross-linking and extended network

formation, resulting in a material that softens at 110 °C but transitions to a thermoset upon further heating. Meanwhile, the 9-phenanthrenyl group induced mainly intramolecular condensation due to its bulkiness, forming rigid, cage-like structures with limited flow behavior.

The incorporation of naphthyl groups into polysilsesquioxanes enables the creation of materials with high refractive indices >1.6, fluorescence, and thermoplastic properties across a wide temperature range while maintaining high thermal stability >400 °C. These characteristics distinguish them from known phenyl-based melting gels, broadening their potential applications in fields like optoelectronics.

## ASSOCIATED CONTENT

### Supporting Information

The Supporting Information is available free of charge at <https://pubs.acs.org/doi/10.1021/acs.macromol.4c02737>.

Experimental section including used materials, instrumentation, and monomer synthesis, spectroscopic data of monomers and formed intermediates during synthesis, spectroscopic data, deconvoluted <sup>29</sup>Si CP-MAS NMR spectra, RI measurements, and TG-FTIR spectra of the prepared polymers (PDF)

## AUTHOR INFORMATION

### Corresponding Author

Guido Kickelbick – *Inorganic Solid-State Chemistry, Saarland University, 66123 Saarbrücken, Germany; Saarene, Saarland Center for Energy Materials and Sustainability, 66123 Saarbrücken, Germany; [orcid.org/0000-0001-6813-9269](https://orcid.org/0000-0001-6813-9269); Email: [guido.kickelbick@uni-saarland.de](mailto:guido.kickelbick@uni-saarland.de)*

### Authors

Svenja Pohl – *Inorganic Solid-State Chemistry, Saarland University, 66123 Saarbrücken, Germany*

Markus Gallei – *Polymer Chemistry, Saarland University, 66123 Saarbrücken, Germany; Saarene, Saarland Center for Energy Materials and Sustainability, 66123 Saarbrücken, Germany; [orcid.org/0000-0002-3740-5197](https://orcid.org/0000-0002-3740-5197)*

Complete contact information is available at: <https://pubs.acs.org/10.1021/acs.macromol.4c02737>

### Notes

The authors declare no competing financial interest.

**Declaration of AI and AI-Assisted Technologies in the Writing Process** During the preparation of this work, the authors utilized AI tools, including [DeepL.com](https://www.deep.com) and ChatGPT to enhance the clarity of the language and to correct spelling, punctuation, and grammatical errors. After using these tools, the authors carefully reviewed and edited the content as necessary and take full responsibility for the accuracy and integrity of the publication.

## ACKNOWLEDGMENTS

Instrumentation and technical assistance for this work were provided by the Service Center X-ray Diffraction, with financial support from Saarland University and the German Science Foundation (project number INST 256/349-1). The authors thank Blandine Boßmann for recording and analyzing the SEC measurements, Elias Gießelmann for MAS NMR measurements, Dr. Alexander Schießer (Department of Chemistry, Mass Spectrometry, Technische Universität Darmstadt) for the

MALDI-ToF MS measurements, and also the Deutsche Forschungsgemeinschaft (Grant INST 163/445-1 FUGG).

## REFERENCES

- (1) Niemczyk, A.; Dziubek, K.; Sacher-Majewska, B.; Czaja, K.; Czech-Polak, J.; Oliwa, R.; Lenza, J.; Szolyga, M. Thermal Stability and Flame Retardancy of Polypropylene Composites Containing Siloxane-Silsesquioxane Resins. *Polymers* **2018**, *10* (9), 1019.
- (2) Park, S.; Jeong, H.-J.; Moon, J.-H.; Jang, E.-Y.; Jung, S.; Choi, M.; Choi, W.; Park, K.; Ahn, H.-W.; Hong, J. Polysilsesquioxane with potent resistance to intraoral stress: Functional coating material for the advanced dental materials. *Appl. Surf. Sci.* **2022**, *578*, No. 152085.
- (3) Hwang, S. O.; Lee, A. S.; Lee, J. Y.; Park, S.-H.; Jung, K. I.; Jung, H. W.; Lee, J.-H. Mechanical properties of ladder-like polysilsesquioxane-based hard coating films containing different organic functional groups. *Prog. Org. Coat.* **2018**, *121*, 105–111.
- (4) Xi, K.; He, H.; Xu, D.; Ge, R.; Meng, Z.; Jia, X.; Yu, X. Ultra low dielectric constant polysilsesquioxane films using  $T^8(\text{Me}_4\text{NO})_8$  as porogen. *Thin Solid Films* **2010**, *518* (17), 4768–4772.
- (5) Baney, R. H.; Itoh, M.; Sakakibara, A.; Suzuki, T. Silsesquioxanes. *Chem. Rev.* **1995**, *95*, 1409–1430.
- (6) Ahmed, N.; Fan, H.; Dubois, P.; Zhang, X.; Fahad, S.; Aziz, T.; Wan, J. Nano-engineering and micromolecular science of polysilsesquioxane materials and their emerging applications. *J. Mater. Chem. A* **2019**, *7*, 21577–21604.
- (7) Temnikov, M. N.; Muzafarov, A. M. Polyphenylsilsesquioxanes. New structures—new properties. *RSC Adv.* **2020**, *10* (70), 43129–43152.
- (8) Masai, H.; Takahashi, M.; Tokuda, Y.; Yoko, T. Gel-melting method for preparation of organically modified siloxane low-melting glasses. *J. Mater. Res.* **2005**, *20*, 1234–1241.
- (9) Katagiri, K.; Hasegawa, K.; Matsuda, A.; Tatsumisago, M.; Minami, T. Preparation of Transparent Thick Films by Electro-phoretic Sol–Gel Deposition Using Phenyltriethoxysilane-Derived Particles. *J. Am. Ceram. Soc.* **1998**, *81*, 2501–2503.
- (10) Matsuda, A.; Sasaki, T.; Hasegawa, K.; Tatsumisago, M.; Minami, T. Thermal Softening Behavior of Poly-(phenylsilsesquioxane) and Poly (benzylsilsesquioxane) Particles. *J. Ceram. Soc. Jpn.* **2000**, *108*, 830–835.
- (11) Katagiri, K.; Hasegawa, K.; Matsuda, A.; Tatsumisago, M.; Minami, T. Preparation of Transparent Thick Films by Electro-phoretic Sol-Gel Deposition Using Phenyltriethoxysilane-Derived Particles. *J. Am. Ceram. Soc.* **1998**, *81* (9), 2501–2503.
- (12) Klein, L. C.; Jitianu, A. Organic-Inorganic hybrid melting gels. *J. Sol-Gel Sci. Technol.* **2010**, *55*, 86–93.
- (13) Jitianu, A.; Amatucci, G.; Klein, L. C. Phenyl-Substituted Siloxane Hybrid Gels that Soften Below 140°C. *J. Am. Ceram. Soc.* **2009**, *92*, 36–40.
- (14) Jeong, S.; Ahn, S.-J.; Moon, J. Fabrication of Patterned Inorganic–Organic Hybrid Film for the Optical Waveguide by Microfluidic Lithography. *J. Am. Ceram. Soc.* **2005**, *88* (4), 1033–1036.
- (15) Mena, B.; Takahashi, M.; Tokuda, Y.; Yoko, T. Preparation and properties of polyphenylsiloxane-based hybrid glass films obtained from a non-aqueous coating sol via a single-step dip-coating. *Opt. Mater.* **2007**, *29*, 806–813.
- (16) Kakiuchida, H.; Takahashi, M.; Tokuda, Y.; Masai, H.; Kuniyoshi, M.; Yoko, T. Viscoelastic and structural properties of a phenyl-modified polysiloxane system with a three-dimensional structure. *J. Phys. Chem. B* **2006**, *110*, 7321–7327.
- (17) Yu, D.; Kleemeier, M.; Wu, G. M.; Schartel, B.; Liu, W. Q.; Hartwig, A. A low melting organic-inorganic glass and its effect on flame retardancy of clay/epoxy composites. *Polymer* **2011**, *52*, 2120–2131.
- (18) Jitianu, A.; Doyle, J.; Amatucci, G.; Klein, L. C. Methyl modified siloxane melting gels for hydrophobic films. *J. Sol-Gel Sci. Technol.* **2010**, *53*, 272–279.
- (19) Kuniyoshi, M.; Takahashi, M.; Tokuda, Y.; Yoko, T. OH-Free Phenyl Modified Siloxane Low-Melting Glasses with Ultra Low Saturated Water-Absorption. *J. Ceram. Soc. Jpn.* **2006**, *114* (7), 660–664.
- (20) Jitianu, A.; Doyle, J.; Amatucci, G.; Klein, L. C. In *Methyl-Modified Melting Gels for Hermetic Barrier Coatings*, Proceedings MS&T 2008 Enabling Surface Coating Systems: Multifunctional Coatings, Pittsburgh PA, 2008.
- (21) Kajihara, K.; Suzuki, R.; Seto, R.; Itakura, H.; Ishijima, M. Poly(cyclohexylsilsesquioxane)-Based Hydrophilic Thermoset-Resistant Deep-Ultraviolet-Transparent Glasses with Low Melting Temperatures. *ACS Appl. Mater. Interfaces* **2023**, *15* (26), 31880–31887.
- (22) Aparicio, M.; Jitianu, A.; Rodriguez, G.; Degnah, A.; Al-Marzoki, K.; Mosa, J.; Klein, L. C. Corrosion Protection of AISI 304 Stainless Steel with Melting Gel Coatings. *Electrochim. Acta* **2016**, *202*, 325–332.
- (23) Klein, L. C.; McClarren, B.; Jitianu, A. Silica-Containing Hybrid Nanocomposite “Melting Gels. *Mater. Sci. Forum* **2014**, *783–786*, 1432–1437.
- (24) Jenkins, S.; Sciarone, E.; Klein, L. C. Texturing melting gels for water harvesting. *J. Sol-Gel Sci. Technol.* **2022**, *101* (1), 37–45.
- (25) Steinbrück, N.; Pohl, S.; Kickelbick, G. Platinum free thermally curable siloxanes for optoelectronic application-synthesis and properties. *RSC Adv.* **2019**, *9* (4), 2205–2216.
- (26) Briesenick, M.; Gallei, M.; Kickelbick, G. High-Refractive-Index Polysiloxanes Containing Naphthyl and Phenanthrenyl Groups and Their Thermally Cross-Linked Resins. *Macromolecules* **2022**, *55* (11), 4675–4691.
- (27) Pohl, S.; Janka, O.; Füglein, E.; Kickelbick, G. Thermoplastic Silsesquioxane Hybrid Polymers with a Local Ladder-Type Structure. *Macromolecules* **2021**, *54* (8), 3873–3885.
- (28) Pohl, S.; Kickelbick, G. Influence of alkyl groups on the formation of softenable polysilsesquioxanes. *J. Sol-Gel Sci. Technol.* **2023**, *107*, 329.
- (29) Macan, J.; Tadanaga, K.; Tatsumisago, M. Influence of copolymerization with alkyltrialkoxysilanes on condensation and thermal behaviour of poly(phenylsilsesquioxane) particles. *J. Sol-Gel Sci. Technol.* **2010**, *53* (1), 31–37.
- (30) Macan, J.; Tadanaga, K.; Tatsumisago, M. Softening of Octyl-modified Phenylsilsesquioxanes. *Polimeri* **2011**, *32* (3–4), 112–118.
- (31) Seto, R.; Kanamura, K.; Yoshida, S.; Kajihara, K. Cosolvent-free synthesis and characterisation of poly(phenyl-co-n-alkylsilsesquioxane) and poly(phenyl-co-vinylsilsesquioxane) glasses with low melting temperatures. *Dalton Trans.* **2020**, *49* (8), 2487–2495.
- (32) Matsuda, A.; Sasaki, T.; Hasegawa, K.; Tatsumisago, M.; Minami, T. Thermal Softening Behavior and Application to Transparent Thick Films of Poly(benzylsilsesquioxane) Particles Prepared by the Sol–Gel Process. *J. Am. Ceram. Soc.* **2001**, *84* (4), 775–780.
- (33) Takahashi, K.; Tadanaga, K.; Hayashi, A.; Tatsumisago, M. Substituent effects on the glass transition phenomena of poly-organosilsesquioxane particles prepared by two-step acid–base catalyzed sol–gel process. *J. Ceram. Soc. Jpn.* **2011**, *119* (1387), 173–179.
- (34) Kannengießler, J.-F.; Briesenick, M.; Meier, D.; Huch, V.; Morgenstern, B.; Kickelbick, G. Synthesis and Hydrogen-Bond Patterns of Aryl-Group Substituted Silanediols and -triols from Alkoxy- and Chlorosilanes. *Chem. - Eur. J.* **2021**, *27* (66), 16461–16476.
- (35) Kannengießler, J.-F.; Morgenstern, B.; Janka, O.; Kickelbick, G. Oligo-Condensation Reactions of Silanediols with Conservation of Solid-State-Structural Features. *Chem. - Eur. J.* **2024**, *30* (16), No. e202303343.
- (36) Meier, D.; Huch, V.; Kickelbick, G. Aryl-group substituted polysiloxanes with high-optical transmission, thermal stability, and refractive index. *J. Polym. Sci.* **2021**, *59* (20), 2265–2283.
- (37) Legrand, S.; Kabir, R.; Kärkkäinen, A. New Phenanthrenyl-Substituted Hybrid Organic-Inorganic Polysiloxanes for Optoelectronic Applications. *ChemistrySelect* **2023**, *8* (5), No. e202204271.
- (38) Legrand, S.; Kärkkäinen, A. Design, synthesis, characterization, and aging properties of a new end-capped three-dimensional high-

- refractive index hybrid organic–inorganic polysiloxane. *J. Appl. Polym. Sci.* **2021**, *138* (21), 50467.
- (39) Liu, J.-G.; Ueda, M. High refractive index polymers: fundamental research and practical applications. *J. Mater. Chem.* **2009**, *19* (47), 8907–8919.
- (40) Kurumada, K.-I.; Ashraf, K. M.; Matsumoto, S. Effects of heat treatment on various properties of organic–inorganic hybrid silica derived from phenyltriethoxysilane. *Mater. Chem. Phys.* **2014**, *144* (1), 132–138.
- (41) Allcock, H. R.; Connolly, M. S.; Sisko, J. T.; Al-Shali, S. Effects of organic side group structures on the properties of poly-(organophosphazenes). *Macromolecules* **1988**, *21* (2), 323–334.
- (42) Stutz, H.; Illers, K.-H.; Mertes, J. A generalized theory for the glass transition temperature of crosslinked and uncrosslinked polymers. *J. Polym. Sci., Part B: Polym. Phys.* **1990**, *28* (9), 1483–1498.
- (43) Bandzler, K.; Reuvekamp, L.; Dryzek, J.; Dierkes, W.; Blume, A.; Bielski, D. Influence of Network Structure on Glass Transition Temperature of Elastomers. *Materials* **2016**, *9* (7), 607.
- (44) Dvornic, P. R.; Lenz, R. W. Exactly alternating silarylene-siloxane polymers. 9. Relationships between polymer structure and glass transition temperature. *Macromolecules* **1992**, *25* (14), 3769–3778.
- (45) Schott, G.; Sprung, W. D. Silanole. V. Die thermische Kondensation von Diaryl-silandiolen. *Z. Anorg. Allg. Chem.* **1964**, *333* (1–3), 76–89.
- (46) Shirai, S.; Goto, Y.; Mizoshita, N.; Ohashi, M.; Tani, T.; Shimada, T.; Hyodo, S.-a.; Inagaki, S. Theoretical Studies on Si–C Bond Cleavage in Organosilane Precursors during Polycondensation to Organosilica Hybrids. *J. Phys. Chem. A* **2010**, *114* (19), 6047–6054.
- (47) Kuniyoshi, M.; Takahashi, M.; Tokuda, Y.; Yoko, T. Hydrolysis and polycondensation of acid-catalyzed Phenyltriethoxysilane (PhTES). *J. Sol-Gel Sci. Technol.* **2006**, *39*, 175–183.
- (48) Gunji, T.; Hayashi, Y.; Komatsubara, A.; Arimitsu, K.; Abe, Y. Preparation and properties of flexible free-standing films via polyalkoxysiloxanes by acid-catalyzed controlled hydrolytic polycondensation of tetraethoxysilane and tetramethoxysilane. *Appl. Organomet. Chem.* **2012**, *26* (1), 32–36.
- (49) Bain, A. D.; Eaton, D. R.; Hamielec, A. E.; Mlekuz, M.; Sayer, B. G. Line broadening in the carbon-13 NMR spectra of crosslinked polymers. *Macromolecules* **1989**, *22* (9), 3561–3564.
- (50) Borovin, E.; Callone, E.; Ribot, F.; Diré, S. Mechanism and Kinetics of Oligosilsesquioxane Growth in the In Situ Water Production Sol–Gel Route: Dependence on Water Availability. *Eur. J. Inorg. Chem.* **2016**, *2016* (13–14), 2166–2174.
- (51) Choi, S.-S.; Lee, A. S.; Hwang, S. S.; Baek, K.-Y. Structural Control of Fully Condensed Polysilsesquioxanes: Ladderlike vs Cage Structured Polyphenylsilsesquioxanes. *Macromolecules* **2015**, *48*, 6063–6070.
- (52) Sen, T.; Bruce, I. J. Surface engineering of nanoparticles in suspension for particle based bio-sensing. *Sci. Rep.* **2012**, *2* (1), No. 564.
- (53) Cabañas, M.; Lozano, D.; Torres-Pardo, A.; Sobrino, C.; González-Calbet, J.; Arcos, D.; Vallet-Regí, M. Features of amino-propyl modified mesoporous silica nanoparticles. Implications on the active targeting capability. *Mater. Chem. Phys.* **2018**, *220*, 260–269.
- (54) Shea, K. J.; Loy, D. A.; Webster, O. Arylsilsesquioxane gels and related materials. New hybrids of organic and inorganic networks. *J. Am. Chem. Soc.* **1992**, *114* (17), 6700–6710.
- (55) Andrianov, K. A.; Izmaylov, B. A. Hydrolytic poly-condensation of higher alkyltrichlorosilanes. *J. Organomet. Chem.* **1967**, *8* (3), 435–441.
- (56) Wallace, W. E.; Guttman, C. M.; Antonucci, J. M. Molecular structure of silsesquioxanes determined by matrix-assisted laser desorption/ionization time-of-flight mass spectrometry. *J. Am. Soc. Mass Spectrom.* **1999**, *10* (3), 224–230.
- (57) Wallace, W. E.; Guttman, C. M.; Antonucci, J. M. Polymeric silsesquioxanes: degree-of-intramolecular-condensation measured by mass spectrometry. *Polymer* **2000**, *41* (6), 2219–2226.
- (58) Chen, X.; Eldred, D.; Liu, J.; Chiang, H.; Wang, X.; Rickard, M. A.; Tu, S.; Cui, L.; LaBeaume, P.; Skinner, K. Simultaneous In Situ Monitoring of Trimethoxysilane Hydrolysis Reactions Using Raman, Infrared, and Nuclear Magnetic Resonance (NMR) Spectroscopy Aided by Chemometrics and Ab Initio Calculations. *Appl. Spectrosc.* **2018**, *72*, 1404–1415.
- (59) Li, Y.-S.; Wang, Y.; Ceesay, S. Vibrational spectra of phenyltriethoxysilane, phenyltrimethoxysilane and their sol-gels. *Spectrochim. Acta, Part A* **2009**, *71*, 1819–1824.
- (60) Newton, W. E.; Rochow, E. G. Vibrational spectra of some trialkoxysilanes. *J. Chem. Soc. A* **1970**, 2664–2668.
- (61) Brown, J. F. The Polycondensation of Phenylsilanetriol. *J. Am. Chem. Soc.* **1965**, *87*, 4317–4324.
- (62) Orel, B.; Ješe, R.; Vilčnik, A.; Štangar, U. L. Hydrolysis and Solvolysis of Methyltriethoxysilane Catalyzed with HCl or Trifluoroacetic Acid: IR Spectroscopic and Surface Energy Studies. *J. Sol-Gel Sci. Technol.* **2005**, *34* (3), 251–265.
- (63) Tagliazucca, V.; Callone, E.; Diré, S. Influence of synthesis conditions on the cross-link architecture of silsesquioxanes prepared by in situ water production route. *J. Sol-Gel Sci. Technol.* **2011**, *60* (3), 236–245.
- (64) Unno, M.; Alias, S. B.; Saito, H.; Matsumoto, H. Synthesis of Hexasilsesquioxanes Bearing Bulky Substituents: Hexakis((1,1,2-trimethylpropyl)silsesquioxane) and Hexakis(tert-butylsilsesquioxane). *Organometallics* **1996**, *15* (9), 2413–2414.
- (65) Sassi, Z.; Bureau, J. C.; Bakkali, A. Spectroscopic study of TMOS–TMSM–MMA gels: Previously identification of the networks inside the hybrid material. *Vib. Spectrosc.* **2002**, *28* (2), 299–318.
- (66) Ishida, H.; Koenig, J. L. Vibrational Assignments of Organosilanetriols. II. Crystalline Phenylsilanetriol and Phenylsilanetriol-D3. *Appl. Spectrosc.* **1978**, *32* (5), 469–479.
- (67) Korkin, S. D.; Buzin, M. I.; Matukhina, E. V.; Zherlitsyna, L. N.; Auner, N.; Shchegolikhina, O. I. Phenylsilanetriol-synthesis, stability, and reactivity. *J. Organomet. Chem.* **2003**, *686* (1), 313–320.
- (68) Hu, N.; Rao, Y.; Sun, S.; Hou, L.; Wu, P.; Fan, S.; Ye, B. Structural Evolution of Silica Gel and Silsesquioxane Using Thermal Curing. *Appl. Spectrosc.* **2016**, *70*, 1328–1338.
- (69) Ye, M.; Wu, Y.; Zhang, W.; Yang, R. Synthesis of incompletely caged silsesquioxane (T<sub>7</sub>-POSS) compounds via a versatile three-step approach. *Res. Chem. Intermed.* **2018**, *44*, 4277–4294.
- (70) Ren, Z.; Xie, P.; Jiang, S.; Yan, S.; Zhang, R. Study of the supramolecular Architecture-Directed synthesis of a Well-Defined Triple-Chain ladder polyphenylsiloxane. *Macromolecules* **2010**, *43*, 2130–2136.
- (71) Yu-zhong, F.; Sheng-li, Q.; Jing-jing, L.; Zhan-peng, W.; Xiaoping, Y.; Ri-guang, J.; De-zhen, W. Preparation and Characterization of Ordered Ladder Like Polyphenylsilsesquioxane via Two-step Sol-gel Method. *Chem. Res. Chin. Univ.* **2011**, *27*, 516–519.
- (72) Xinsheng, Z.; Lianghe, S.; Chaoran, H. More on the Structures of Polyphenylsilsesquioxanes. *Chin. J. Polym. Sci.* **1987**, *5*, 353–358.
- (73) Kang, W. R.; Lee, A. S.; Park, S.; Park, S. H.; Baek, K.-Y.; Lee, K. B.; Lee, S.-H.; Lee, J.-H.; Hwang, S. S.; Lee, J. S. Free-standing polysilsesquioxane-based inorganic/organic hybrid membranes for gas separations. *J. Membr. Sci.* **2015**, *475*, 384–394.
- (74) Papkov, V.; Gerasimov, M. V.; Buzin, M.; Il'ina, M. N.; Kazaryan, L. G. The structure of ordered phases in polydiphenylsiloxane. *Polym. Sci., Ser. A* **1996**, *38*, 1097–1102.
- (75) Liu, F.; Zeng, X.; Lai, X.; Li, H. Synthesis and characterization of polyphenylsilsesquioxane terminated with methyl and vinyl groups low-melting glass. *J. Adhes. Sci. Technol.* **2017**, *31*, 2399–2409.
- (76) Shang, X.; Cao, X.; Ma, Y.; Kumaravel, J. J.; Zheng, K.; Zhang, J.; Zhang, R. Diphenylsiloxane-bridged ladder-like hydrido-polysiloxane and the derivatisation by triphenylsiloxy substitution. *Eur. Polym. J.* **2018**, *106*, 53–62.

- (77) Jovanovic, J. D.; Govedarica, M. N.; Dvornic, P. R.; Popovic, I. G. The thermogravimetric analysis of some polysiloxanes. *Polym. Degrad. Stab.* **1998**, *61* (1), 87–93.
- (78) Camino, G.; Lomakin, S. M.; Lageard, M. Thermal polydimethylsiloxane degradation. Part 2. The degradation mechanisms. *Polymer* **2002**, *43* (7), 2011–2015.
- (79) Xinsheng, Z.; Lianghe, S.; Shuqing, L.; Yizhen, L. Thermal Stability and Kinetics of Decomposition of Polyphenylsilsesquioxanes and Some Related Polymers. *Polym. Degrad. Stab.* **1988**, *20*, 157–172.
- (80) Zhou, W.; Yang, H.; Guo, X.; Lu, J. Thermal degradation behaviors of some branched and linear polysiloxanes. *Polym. Degrad. Stab.* **2006**, *91*, 1471–1475.
- (81) McManus, J. C.; Harano, Y.; Low, M. J. D. Infrared study of the interactions of acetone and siliceous surfaces. *Can. J. Chem.* **1969**, *47* (14), 2545–2554.
- (82) Zhang, D.; Yang, R.; Qin, Z.; Zhang, W. Study on the thermal behaviors of polyhedral oligomeric octaphenylsilsesquioxane (OPS). *J. Therm. Anal. Calorim.* **2023**, *148* (6), 2345–2355.
- (83) Bolln, C.; Tsuchida, A.; Frey, H.; Mülhaupt, R. Thermal Properties of the Homologous Series of 8-fold Alkyl-Substituted Octasilsesquioxanes. *Chem. Mater.* **1997**, *9* (6), 1475–1479.
- (84) Förster, T.; Kasper, K. Ein Konzentrationsumschlag der Fluoreszenz des Pyrens. *Z. Elektrochem. Ber. Bunsenges. Phys. Chem.* **1955**, *59* (10), 976–980.
- (85) Stevens, B.; Hutton, E. Radiative Life-time of the Pyrene Dimer and the Possible Role of Excited Dimers in Energy Transfer Processes. *Nature* **1960**, *186* (4730), 1045–1046.
- (86) Birks, J. B.; Christophorou, L. G.; Flowers, B. H. 'Excimer' fluorescence. IV. Solution spectra of polycyclic hydrocarbons. *Proc. R. Soc. London, Ser. A* **1964**, *277* (1371), 571–582.
- (87) Vala, M. T., Jr.; Haebig, J.; Rice, S. A. Experimental Study of Luminescence and Excitation Trapping in Vinyl Polymers, Paracyclophanes, and Related Compounds. *J. Chem. Phys.* **1965**, *43* (3), 886–897.
- (88) Fox, R. B.; Price, T. R.; Cozzens, R. F.; McDonald, J. R. Photophysical Processes in Polymers. IV. Excimer Formation in Vinylaromatic Polymers and Copolymers. *J. Chem. Phys.* **1972**, *57* (1), 534–541.
- (89) Salom, C.; Horta, A.; Hernandez-Fuentes, I.; Pierola, I. F. Poly(phenylsiloxanes) electronic spectra. *Macromolecules* **1987**, *20*, 696–698.
- (90) Liu, C.; Liu, Y.; Shen, Z.; Xie, P.; Zhang, R.; Yang, J.; Bai, F. Study of the Steric Tacticity of Novel Soluble Ladderlike Poly(phenylsilsesquioxane) Prepared by Stepwise Coupling Polymerization. *Macromol. Chem. Phys.* **2001**, *202*, 1581–1585.
- (91) Hirayama, F. Intramolecular excimer formation. I. Diphenyl and triphenyl alkanes. *J. Chem. Phys.* **1965**, *42*, 3163–3171.
- (92) Aladekomo, J. B.; Birks, J. B. 'Excimer' fluorescence VII. Spectral studies of naphthalene and its derivatives. *Proc. R. Soc. London, Ser. A* **1965**, *284*, 551–565.
- (93) Lewis, F. D.; Burch, E. L. Excimer fluorescence from phenanthrene-9-carboxylate derivatives. *J. Photochem. Photobiol., A* **1996**, *96* (1), 19–23.
- (94) Jones, P. F.; Nicol, M. Excimer Emission of Naphthalene, Anthracene, and Phenanthrene Crystals Produced by Very High Pressures. *J. Chem. Phys.* **1968**, *48* (12), 5440–5447.
- (95) Chandross, E. A.; Thomas, H. T. Excited dimer luminescence of pairs of phenanthrene molecules. *J. Am. Chem. Soc.* **1972**, *94* (7), 2421–2424.
- (96) Chandross, E. A.; Longworth, J. W.; Visco, R. E. Excimer Formation and Emission via the Annihilation of Electrogenerated Aromatic Hydrocarbon Radical Cations and Anions. *J. Am. Chem. Soc.* **1965**, *87* (14), 3259–3260.
- (97) Chaoran, H.; Guangzhi, X.; Xinsheng, Z.; Lianghe, S. Studies on the Excimer Fluorescence and the Steric Tacticity of Polyphenylsilsesquioxanes. *Chin. J. Polym. Sci.* **1987**, *5*, 347–352.
- (98) Belova, A. S.; Kononevich, Y. N.; Sazhnikov, V. A.; Safonov, A. A.; Ionov, D. S.; Anisimov, A. A.; Shchegolikhina, O. I.; Alfimov, M. V.; Muzafarov, A. M. Solvent-controlled intramolecular excimer emission from organosilicon derivatives of naphthalene. *Tetrahedron* **2021**, *93*, No. 132287.
- (99) Chandross, E. A.; Dempster, C. J. Intramolecular excimer formation and fluorescence quenching in dinaphthylalkanes. *J. Am. Chem. Soc.* **1970**, *92* (12), 3586–3593.